CR 137571

AVAILABLE TO THE PUBLIC

COMPUTER EXPERIMENTS IN PREPARATION OF SYSTEM IDENTIFICATION FROM TRANSIENT ROTOR MODEL TESTS

Part II of First Yearly Report under Contract NAS2-7613

Prepared for the Ames Directorate, AMRDL
a' Ames Research Center, Moffett Field, California

by

K. H. Hohenemser

and

S. K. Yin

Department of Mechanical and
Aerospace Engineering

Washington University
School of Engineering and Applied Science
St. Louis, Missouri 63130

June, 1974

(NASA-CR-137571) COMPUTER EXPERIMENTS IN PREPARATION OF SYSTEM IDENTIFICATION FROM TRANSIENT ROTOR MODEL TESTS, PART 2 First Yearly Report (Washington Univ.) 6^ p HC $6.^^ CSCL ^1B G3/^2

N74-34^84

Unclas
^1633

COMPUTER EXPERIMENTS IN PREPARATION OF SYSTEM IDENTIFICATION FROM TRANSIENT ROTOR MODEL TESTS

Part II of First Yearly Report under Contract NAS2-7613

Prepared for the Ames Directorate, AMRDL
at Ames Research Center, Moffett Field, California

by

K. H. Hohenemser

and

S. K. Yin

Department of Mechanical and
Aerospace Engineering

Washington University
School of Engineering and Applied Science
St. Louis, Missouri 63130

June, 1974

Preface to First Yearly Report under Contract NAS2-7613

Work under Contract NAS2-7613 started on July 1, 1973. It is a continuation of research conducted since February 1, 1967, under Contract NAS2-4151. Phase VII-A, B and C Reports of June, 1973, titled, "Concepts for a Theoretical and Experimental Study of Lifting Rotor Random Loads and Vibrations", are the final reports under Contract NAS2-4151 and list the 9 preceding reports and 11 published articles and papers prepared under the contract.

Meanwhile 2 further papers generated under this Contract have been published:

Crews, S. T., Hohenemser, K. H. and Ormiston, R. A., "An Unsteady Wake Model for a Hingeless Rotor", Journal of Aircraft Vol. 10, No. 12, Dec. 1973, pp. 758-760.

Hohenemser, K. H. and Prelewicz, D. A., "Computer Experiments on Periodic Systems Identification Using Rotor Blade Transient Flapping-Torsion Responses at High Advance Ratio", AHS/NASA Ames Specialists Meeting on Rotorcraft Dynamics, Moffett Field, California, February 1974.

The first paper which has been generated under the new Contract NAS2-7613 is:

Hohenemser, K. H. and Yin, S. K., "On the Use of First Order Rotor Dynamics in Multiblade Coordinates", presented at the 30th Annual National Forum of the American Helicopter Society, May 1974, Preprint 831.

The research goals stated in Contract NAS2-7613 are

(a) Assess analytically the effects of fuselage motions on stability and random response. The problem is to develop an adequate but not overly complex flight dynamics analytical model and to study the effects of structural and electronic feedback, particularly for hingeless rotors.

(b) Study by computer and hardware experiments the feasibility of adequate perturbation models from non-linear trim conditions. The problem is to extract an adequate linear perturbation model for the purpose of stability and random motion studies. The extraction is to be performed on the basis of transient responses obtained either by computed time histories or by model tests.

(c) Extend the experimental methods to assess rotor wake-blade interactions by using a 4-bladed rotor model with the capability of progressing and regressing blade pitch excitation (cyclic pitch stirring), by using a 4-bladed rotor model with hub tilt stirring, and by testing rotor models in sinusoidal up or side flow.

The first yearly report under Contract NAS2-7613 is subdivided into 3 parts, whereby Parts I, II, and III are related to the research goals (a), (b), and (c) respectively. The authors and titles of the three parts are:

Part I, Hohenemser, K. H. and Yin, S. K., "Methods Studies Toward Simplified Rotor-Body Dynamics".

Part II, Hohenemser, K. H. and Yin, S. K., "Computer Experiments in Preparation of System Identification from Transient Rotor Model Tests".

Part III, Hohenemser, K. H. and Crews, S. T., "Experiments with a Four-Bladed Cyclic Pitch Stirring Model Rotor".

Part I considers a number of simplifications in rotor-body dynamics and applies the various analytical models to a hypothetical compound hingeless rotorcraft with and without feedback into cyclic and collective controls.

Part II deals with the problem of rotor parameter identification from noise polluted transient blade flapping responses. Computer experiments are used in order to gain some insight into the efficiency of various identification schemes to be later applied to rotor model flapping transients.

Part III summarizes the test results obtained with the 4-bladed cyclic pitch stirring model rotor. The analytical blade flapping responses without considering the rotor wake are compared to the measured responses which include the wake-blade interactions.

IV

COMPUTER EXPERIMENTS IN PREPARATION OF SYSTEM IDENTIFICATION FROM TRANSIENT ROTOR MODEL TESTS

Part II of First Yearly Report under Contract NAS2-7613

Abstract

This report is directed to the problem of developing system identification methods which can extract model rotor parameters with reasonable accuracy from noise polluted blade flapping transient measurements. Usually parameter identification requires data on the state variables, that is on deflections and on rate of deflections. The small size of rotor models makes it, however, difficult to measure more than the blade flapping deflections. For the computer experiments it was, therefore, assumed that only noisy deflection measurements are available. Parameter identifications were performed for one and two unknown parameters. Both rotating coordinates and multiblade coordinates were used. It was found that data processing with a digital filter allowed by numerical differentiation a sufficiently accurate determination of the rates of deflection and of the accelerations to obtain reasonable parameter estimates with a simple linear estimator. The estimates could be improved by computing the rates of deflection and the accelerations with a Kalman filter based on the system equations with the first estimate of the parameters.

COMPUTER EXPERIMENTS IN PREPARATION OF SYSTEM IDENTIFICATION FROM TRANSIENT ROTOR MODEL TESTS

Part II of First Yearly Report under Contract NAS2-7613

<u>Table of Contents</u>

Nomenclature

a	parameter vector
$C(t)$	time variable blade flap damping
$F(x,a)$	system function
F	system matrix
G	system input gain matrix
$H(x)$	measurement function
H	measurement matrix
$K(t)$	time variable aerodynamic blade stiffness
m_λ	aerodynamic λ derivative
P_x	state covariance matrix
P_a	parameter covariance matrix
P	covariance matrix, if reference to x or a is unambiguous
Q	system input noise covariance matrix
R	measurement noise covariance matrix
t	non-dimensional time in which period of rotor revolution is 2π
v	measurement noise vector
w	system input vector including input noise
x	state vector
z	measurement vector
β	blade flapping angle
γ	blade Lock number
δ	$\gamma\theta_o$
θ_o	blade collective pitch angle

λ	non-dimensional normal flow velocity, or variable for backward sweep
μ	rotor advance ratio
σ	standard deviation
ω_1	rotating blade flapping natural frequency

Subscripts

o	value at time t = 0, or cellective
1,2	first, second state variable
I,II	first, second multiblade variable for forward and left cyclic flapping respectively

Superscripts

$-$	mean value
$\hat{}$	estimated value
T	transpose
-1	inverse
$\cdot$	time derivative

Introduction

The method of System Identification is becoming an efficient analytical tool to correlate a set of system equations with transient responses obtained either experimentally or from a time history of a more complete analytical model of the system. The method of system identification is particularly effective if a linear perturbation model of a basically non-linear system is to be identified. Applications of system identification methods to V/STOL aircraft are described in Reference [1], applications to rotorcraft are described in Reference [2], and computer experiments toward single blade system identification at high advance ratio are reported in Reference [3].

For a linearized system of perturbation rotor equations the frequency response functions or transfer functions completely describe the system. For hingeless rotor models such functions have been experimentally determined, see Reference [4] and Part III of this report. Reference [5] presents correlations of the frequency responses with analytical models. Since both the rotor frequency response testing and the correlation with analytical rotor models is quite laborious, an attempt will be made to extract an adequate linear perturbation model from transient rotor responses. This is in accordance with Research Goal (b) stated in the Preface. The analytical model will be the simpler, the smaller the frequency range which it is required to cover. In an inertial system the lowest rotor natural frequency, that of the regressing blade flapping mode, is widely separated from the higher natural frequencies, those of the coning and advancing blade flapping modes. From Reference [5] one can expect that in this low frequency range the quasisteady inflow assumption will be a reasonable approximation.

The simplest inflow representation is that by an equivalent blade Lock number. In a more sophisticated inflow representation the "L" matrix of References [5] and [6] can be used. As explained in Part III of this report the rotor model excitation will first consist of transients of cyclic pitch stirring. After completion of the test equipment to generate sinusoidal normal flow variations in the wind tunnel, excitations with normal flow transients will be possible. In this report we are concerned about the identification of the blade Lock number from rotor responses to transient normal flow inputs.

The work reported in the following is of a preliminary nature and was intended to gain some experience with a number of identification schemes applied to lifting rotors. Normal flow transients were used in two forms: The first is a rectangular normal flow pulse, the second a wave shaped normal flow pulse. In either case it is assumed that the entire rotor disk experiences at a given instant of time the same normal flow velocity. Though this assumption is not very realistic, particularly for the rectangular pulse, it was used because of its convenience, since the emphasis was on the identification methods, not the actual identifications. The transients were obtained with a complete linear analysis including periodic terms. For the identification two analytical models were used: A complete blade representation in a rotating frame of reference, and a simplified multiblade representation omitting periodic terms and omitting the multiblade accelerations.

The computer experiments in this report differ in their basic assumptions from those of Reference [3]. In earlier computer experiments it was assumed that ・ ・e polluted measurements of the blade flapping and t sional blade deflections, rate of deflections and accelerations are available, and that the trim responses have been removed. The parameter identification was thus based on pure transient responses to normal flow pulses. In this report it was assumed that only noise polluted blade flapping deflections are known, not their rates or accelerations, since this will be the situation in the planned transient rotor model tests. It was also assumed in some of the computer experiments, that transient and trim responses had not been separated, which requires the identification of two parameters. Because of the torsionally very stiff model rotor blades and the relatively low advance ratio assumed here (μ = .4), torsional elasticity and reversed flow effects could be omitted.

Non-linear Simultaneous State and Parameter Estimation

The general problem of estimating rotorcraft derivatives from noisy measurements of transients which include the effects of unknown turbulence excitation is defined in Reference [2] and developed in more detail in Reference [7]. The characterization in Reference [2] as "Bayesian Approach to Estimation" is meant to emphasize a certain interpretation of the identification algorithm rather than a specific "Bayesian" algorithm. The same algorithm can also be interpreted as expression of maximization of a performance criterion.

The general problem is the following: Given the non-linear process or system equations with an unknown constant parameter vector a, unknown state vector x and known or unknown system input vector w, including input noise

$$\dot{x} = F(x,a) + G\,w \quad , \tag{1}$$

whereby $\dot{a} = 0$ (2)

and given the measurement equations relating the state vector to the measurement vector z with the random measurement noise vector v,

$$z = H(x) + v \tag{3}$$

determine the estimates at time t = 0 for the state vector and for the parameter vector $\hat{x}_o$ and $\hat{a}_o$ respectively such that the conditional probability density function p(x/z) of the state given the measurement is maximized for each time step. The estimate $\hat{a}_o$ represents the optimal constant parameter vector.

In terms of the performance criterion the solution requires maximization of the expression

$$J = (1/2)\{(\hat{a}_o-a_o)^T P_{a_o}^{-1} (\hat{a}_o-a_o) + (\hat{x}_o-x_o)^T P_{x_o}^{-1} (\hat{x}_o-x_o) + \int_o^t (w-\overline{w})^T Q^{-1}(w-\overline{w})dt + \int_o^t (z-H(x))^T R^{-1}(z-H(x))dt\} \tag{4}$$

where a_o and x_o are the estimates of parameter and state vector at time t = 0 before the measurements, and where P_{a_o} and P_{x_o} are the corresponding covariance matrices before the measurements.

Parameters and state variables appear as products in the system function F(x,a). In maximizing the expression Eq. (4) one obtains a set of non-linear differential equations for the estimates $\hat{x}$ and $\hat{a}$ which are given in a form suitable for application to rotorcraft identification in Reference [7]. One problem of the simultaneous estimation of state vector and parameter vector is its sensitivity to the initial estimates before measurements x_o, a_o. Unless one has reasonably good initial estimates the non-linear estimation algorithm may grossly diverge. The quality of the estimate also depends on the quality of the analytical model used in the identification algorithm, that is it depends on the possible modeling errors. Furthermore, the transient used in the identification scheme must be within the range of validity of the linear perturbation model. For large amplitude transients with substantial non-linear effects one cannot expect a valid identification of a linear perturbation model. And, finally, the quality of the estimation depends on the character of the transient which must involve all essential modes of the linear perturbation model. If such "global" transients are not available, one can use a sequence of specialized transients which in combination excite all essential modes of the perturbation model. If the transients are too short for an effective parameter identification, one can use a sequence of transients of the same type and introduce for each additional transient a new set of state variables and parameters. All sets are identified simultaneously whereby the mean value over the set of parameters represents an improved estimate as compared to that obtained from a single transient, see References [2] and [7]. An identification method for the special case of steady random system excitation is given in Reference [8]. Parameters and states are estimated simultaneously by a non-linear algorithm, making use of a Kalman filter representation of the system.

Linear State Estimation

Linear estimators are obtained if one assumes that either the parameter vector a or the state vector x is known. In the first case the first term in Eq. (4) is zero. Maximization of the remaining expressions in Eq. (4) leads to the linear extended Kalman filter equations for the estimate $\hat{x}$, see for example Reference [9].

$$\dot{\hat{x}} = F(\hat{x}) + G\bar{w} + P\left(\frac{\partial H}{\partial x}\right)^T R^{-1}(z - H(\hat{x})) \tag{5}$$

$$\dot{P} = \frac{\partial F}{\partial x} P + P\left(\frac{\partial F}{\partial x}\right)^T + GQG^T - P\left(\frac{\partial H}{\partial x}\right)^T R^{-1} \frac{\partial H}{\partial x} P \tag{6}$$

P stands here for P_x. For a linear perturbation model $F(\hat{x})$ and $H(\hat{x})$ are linear functions of the estimate $\hat{x}$ and can also be written as $F\hat{x}$ and $H\hat{x}$ respectively, where F is the system matrix and H the measurement matrix. Initial estimates before measurements of state vector x_o and its associated covariance matrix P_o must be made, and the quality of the estimate $\hat{x}$ vs. time will depend on the quality of these initial estimates. The covariance Eq. (6) can be integrated without knowing $\hat{x}$ or z. In the absence of system noise, Q = 0, P may asymptotically approach zero. From then on the solution of the filter Eq. (5) will not depend anymore on the measurements z. The estimate $\hat{x}$ is then identical to the result from integrating the system Eq. (1)

for given a. As long as P is finite, the integration of the system equation will result in a state vector x different from $\hat{x}$ due to the third term in Eq. (5). For large measurement noise the correction term from measurements in Eq. (5) will have little effect on the estimate $\hat{x}$, since the correction term has a factor R^{-1}.

If all state variables are measured without noise, Eq. (5) reverts to the system equation (1) and there is no need for the Kalman filter. If there are noisy measurements of some state variables and no measurements of other state variables, Eqs. (5) and (6) will provide an optimal estimate of all state variables given the measurements. If not all parameters of the vector a are well known, and if only incomplete noisy measurements of x exist, one can still use Eqs. (5) and (6) to obtain an estimate $\hat{x}$, on the condition that the errors in a are not substantial. This case will be treated in one of the later numerical examples.

The estimate $\hat{x}(t)$ from Eqs. (5) and (6) is optimal given the measurements z between time 0 and time t. For small time values the estimate will be less accurate than for larger time values, since fewer measurement data are used. One method of improving the early estimates by utilizing all of the measurement data is smoothing by the backward sweep method, see for example Reference [9]. Once $\hat{x}$ is known from

Eqs. (5) and (6) up to $t = t_f$, one determines for the linear case $H(x) = Hx$, $F(x) = Fx$ the variable λ from

$$\dot{\lambda} = -(F-PH^TR^{-1}H)^T\lambda + H^TR^{-1}(z - H\hat{x}) \tag{7}$$

integrating backwards with initial condition $\lambda(t_f) = 0$. The improved estimate $\hat{\hat{x}}$ of the state vector is

$$\hat{\hat{x}} = \hat{x} - P\lambda \tag{8}$$

which is optimal given all measurements between $t = 0$ and $t = t_f$. One can now also improve on the mean value of the system input which had been assumed as $\overline{w}$ before measurements. The optimal estimate $\hat{w}$ given all measurements is

$$\hat{w} = \overline{w} - QG^T\lambda \tag{9}$$

In this report we will not make use of the possibility of improving the early estimate from Eqs. (5) and (6) by the process of smoothing, but this possibility should be looked into for later lifting rotor applications.

Another way of using Eqs. (5) and (6), documented for exampl in Reference [7], is to replace the system Eq. (1) by a relation between the state variables and the acceleration which does not include the parameter vector a. Assuming, for example, that noisy acceleration measurements exist, one writes Eq. (1) in the form

$$\dot{x} = Gw \tag{10}$$

whereby w is now a measured quantity. In addition we have the measurements z. Eqs. (5) and (6) for $F(\hat{x}) = 0$ allow now to determine an optimal estimate $\hat{x}$ based on the measurements, without knowing the system equation. Such data processing is desirable before parameter identification. In the case of our planned model tests this type of data processing is not possible since only flapping deflections are measured but not deflection rates or accelerations. Mathematical relations between measured quantities outside the system equations do, therefore, not exist.

Linear Parameter Estimation

We are now proceeding to the second case of a linear estimation where we assume that by measurements and data processing the state vector x and its derivative $\dot{x}$ are known, while the parameter vector a is unknown. We replace the system equation by Eq. (2), and write the measurement Eq. (3) in the form of the system equation

$$z = \dot{x} = H(x,a) + v \tag{11}$$

The optimal estimate $\hat{a}$ based on measurements $\dot{x}$ and x is now given by Eqs. (5) and (6) after replacing $\hat{x}$ by $\hat{a}$ and considering $F(\hat{a}) = \overline{w} = Q = 0$.

$$\dot{\hat{a}} = P\left(\frac{\partial H}{\partial a}\right)^T R^{-1}[z - H(x,a)] \tag{12}$$

$$\dot{P} = -P\left(\frac{\partial H}{\partial a}\right)^T R^{-1} \frac{\partial H}{\partial a} P \tag{13}$$

P stands here for P_a. Since asymptotically, when the transient has subsided, $P \rightarrow 0$, $\dot{\hat{a}} \rightarrow 0$, one obtains asymptotic values for the parameter vector estimate. While noise in the acceleration measurement of $\dot{x}$ is of no concern - Eq. (11) includes the noise term v -, there is no provision in this algorithm for noise in the state vector measurement x. As shown in Reference [1] and as will become obvious also from the later numerical examples, noise in the measurement of x produces a bias in the estimate $\hat{a}$, same as non-linearities in the system equations. It is, therefore advisable, before applying the parameter estimation scheme of Eqs. (12) and (13), to remove as much as possible the noise in the state variable measurements.

The simultaneous estimation of state variables and parameters by non-linear algorithms like those used in References [7] and [8] requires good initial estimates to start up the algorithm. A linear estimator like Eqs. (12) and (13) can provide these initial estimates with little effort. The question then is, whether the improvements possible with the non-linear estimators are worth the considerable additional effort. In the following computer experiments only the linear estimator Eqs. (12) and (13) was applied.

In all cases parameters could be identified with only a few percent error, so that an improvement of the estimate was unnecessary. The situation may change when more complex rotor identification problems will be attacked in the future.

Parameter Estimation from Single Blade Response

From an experimental point of view, the blade flapping response to a transient input is easy to obtain in a rotating reference system. In addition to the transient blade flapping motion there is the flapping motion from trim, which can be much larger than the transient. The inaccuracies involved in separating out the transient from the combined transient and trim response may be significant. As an alternative it will be attempted to identify the blade Lock number from the combined response.

The first transient model experiments are expected to be conducted with transients in cyclic pitch stirring frequency. Later experiments will be made with transient normal flow variations. The computer experiments reported here all refer to normal flow transients. It is assumed that the entire rotor disk experiences at a given time the same normal flow component. This simplified model is believed to be adequate to provide some insight into the accuracy of the various identification schemes. For the later actual identifications from experimental normal flow transients a better analytical model considering the gradual penetration of the rotor disk into a normal flow wave may become necessary.

The two transient excitations studied are a rectangular pulse and a wave shaped pulse of normal flow. They are shown in Fig. 1 together with their flapping responses in the rotating reference system. The response is obtained from the linear analysis assuming a blade Lock number of $\gamma = 5$, a rotating blade natural frequency of $\omega_1 = 1.2$, and an advance ratio of $\mu = .4$. (The tip loss factor is .97) A straight rigid blade elastically hinged at the rotor center was assumed.

Identification with Eqs. (12) and (13) requires data on deflections, rate of deflections and accelerations, that is x and $\dot{x}$ must be known. The rates of deflection and the accelerations can either be obtained from the solution of the response problem, or by numerical differentiation of the deflection response. If the latter is not noise polluted it was found that either method is satisfactory and leads to the same estimates. The identification of the blade Lock number has been performed for 4 types of responses:

1. Unpolluted transient
2. Noise polluted transient
3. Unpolluted combined transient and trim response
4. Noise polluted combined transient and trim response

Estimation from Unpolluted Response

We begin with the first type. The question arises, what initial conditions $\hat{\gamma}_o$ and P_o to select. In order to cover the most unfavorable case, $\hat{\gamma}_o = 0$ was selected in all examples.

The accuracy of the estimate can be improved, though not by much, if a better initial estimate is used, say $\hat{\gamma}_o = 3$, where actually $\gamma = 5$. With respect to the initial value P_o it was found that the accuracy of the estimate was usually better for higher values of P_o. An upper limit of P_o is given by the selected time step for the numerical integration of Eq. (13). $\dot{P}$ is negative and should not be so large as to reduce P excessively for one time step. These time steps were selected to be .1 in a non-dimensional time which makes the period of one rotor revolution 2π.

Fig. 2(a) shows for the rectangular normal flow pulse the estimate $\hat{\gamma}$ and its covariance P vs. time for $P_o = 1000$ and 2000. The final value of $\hat{\gamma}$ is obtained after less than one rotor revolution. The higher initial covariance gives the better estimate which has an error of about 2%. Fig. 2(b) shows for the wave shaped normal flow pulse the estimate $\hat{\gamma}$ and its covariance P. Now the asymptotic value of $\hat{\gamma}$ is delayed to somewhat less than 2 rotor revolutions. Again the higher initial covariance gives the better estimate. Because of the slow build-up of the flapping transient evident from Fig. 1(b) the identification takes longer and is for the same initial value of P_o less accurate. As the curve for $P_o = 5000$ shows, a better accuracy of about 1% can be obtained for a higher initial P_o. The higher values of P_o for the wave shaped pulse as compared to the rectangular pulse are admissable since the maximum down slopes of the P curves are much lower for the wave shaped pulse.

Estimation from Noise Polluted Digitally Filtered Response

We now proceed to the second type of response, the noise polluted transient. Simulated noisy measurements were obtained by adding at each of the time points used for the numerical integration (time step size .1) samples from zero mean computer generated Gaussian random sequences. Contrary to Reference [3] the noise was only added to the computed blade flapping deflections. The problem now is, how to best obtain the rates of deflection and the accelerations needed for the identification algorithm of Eqs. (12) and (13). Kalman filtering of the data without using the system equations, as was performed in Reference [7], is not possible here, since no mathematical relations between the test data outside the system equations exist. One way is to filter the data with a zero phase shift digital filter and then differentiate the filtered data twice for insertion into Eqs. (12) and (13). In selecting the cut-off frequency of the digital filter, one wishes to remove the noise without distorting the response too much. Three cut-off ranges of the digital filter (see Reference 10) were tried: .6 to .9, 1.7 to 1.9, 3.5 to 3.9.

It was found that the accuracy of the parameter identification is best for the middle range. The standard deviation of the added white noise was $\sigma_\beta = .2$ and is pictured in Fig. 1

in comparison to the response curves. This is a substantially higher noise level than can be expected in the rotor model measurements. A value of σ_β = .05 was also investigated. The initial value of the covariance was P_o = 2000.

Figs. 3(a) and 3(b) show for P_o = 2000 the estimate $\hat{\gamma}$ and it variance P/P_o for the rectangular and wave shaped pulse respectively. The cases σ_β = .2 and .05 are presented. For the rectangular pulse the error in the final estimate is much larger than for the unpolluted case, as can be seen by comparing Figs. 2(a) and 3(a). The error is about 12% for σ_β = .05 and 16% for σ_β = .2 as compared to 2% when using the unpolluted transient. For the wave shaped pulse the errors in the estimate are little affected by the noise pollution, as can be seen by comparing Figs. 2(b) and 3(b) for P_o = 2000. For σ_β = .05 the error is about 4%, for σ_β = .2 it is twice as large. Due to the noise pollution the $\hat{\gamma}$ curves do not have an asymptote within the time range shown up to t = 12, but fluctuate to a certain degree. The reason why noise pollution has a lower effect on the accuracy of the estimate for the wave shaped pulse is probably the more gradual onset of the response which leads to smaller initial errors in the differential quotients of the noise polluted filtered response. Fig. 4 shows for the two types of normal flow pulses the rate of blade flapping deflection with and without noise pollution obtained by differentiating the noise polluted and filtered response. There is for both types of pulses a sizeable error in $\dot{\beta}$ from noise pollution which is magnified after another differentiation to obtain $\ddot{\beta}$.

Improved Estimation from Kalman Filtered Response

Once an approximate value for the parameter is known, one can attempt to improve on the result of the identification by applying the Kalman filter Eqs. (5) and (6) to the measured response, using the approximation for the parameter. One can either apply the Kalman filter directly to the noisy data, or one can first smooth the data with a digital filter as was done before. It was found that the second method is the better one, if one ignores the Kalman filter result with respect to $\hat{\beta}$ and only uses $\hat{\dot{\beta}}$ and $\hat{\ddot{\beta}}$ from the Kalman filter. In other words, rather than numerically differentiating the digitally filtered deflection function β, one lets the Kalman filter with the approximate value of the parameter γ perform the differentiation.

The system and measurement equations corresponding to Eqs. (5) and (6) are

$$\begin{bmatrix} \dot{x}_1 \\ \dot{x}_2 \end{bmatrix} = \begin{bmatrix} 0 & 1 \\ (\gamma/2)K(t)+\omega_1^2 & (\gamma/2)C(t) \end{bmatrix} \begin{bmatrix} x_1 \\ x_2 \end{bmatrix} + \begin{bmatrix} 0 & 0 \\ 0 & -(\gamma/2)m_\lambda \end{bmatrix} \begin{bmatrix} 0 \\ \lambda \end{bmatrix} \tag{14}$$

$$\begin{bmatrix} z_1 \\ z_2 \end{bmatrix} = \begin{bmatrix} 1 & 0 \\ 0 & 0 \end{bmatrix} \begin{bmatrix} x_1 \\ x_2 \end{bmatrix} \tag{15}$$

where $x_1 = \beta$, $x_2 = \dot{\beta}$. It was found that the Kalman filter with the digitally filtered measurements yields better values $\dot{\beta}$, $\ddot{\beta}$ than the direct numerical differentiations, though γ is in error.

The method was applied to the case of Fig. 3(a) where with $\sigma_\beta = .2$ the final estimate was $\hat{\gamma} = 4.2$. This value was inserted into the Kalman filter equations rather than the correct value $\gamma = 5.0$. A unity matrix was assumed for R, since for Q = 0 and R diagonal the solution does not depend on the individual P and R but only on PR^{-1}. After setting R = I the initial value of P was selected as

$$P_o = \begin{bmatrix} 2 & 0 \\ 0 & 2 \end{bmatrix} \tag{16}$$

This is the highest value consistent with the requirement that the initial slope $\dot{P}_o$ does not result in an excessive change of the components of P over the time increment $\Delta t = .1$. At first an initial covariance matrix

$$P_o = \begin{bmatrix} 10 & 0 \\ 0 & 10 \end{bmatrix} \tag{16a}$$

had been selected. The reduction of P_{11} during the first time increment was $\Delta P_{11} = 9$, which is clearly excessive. The diagonal terms of the covariance matrix obtained by numerically integrating Eq. (6) are shown in Fig. 5.

Fig. 6 shows a comparison of the flapping rates and accelerations between the exact values ($\sigma_\beta = 0$), the values obtained from numerical differentiation of the filtered polluted β data, and the values from the Kalman filter with $\gamma = 4.2$ instead of $\gamma = 5.0$. It is evident, how much better the Kal .an filter values for $\dot{\beta}$ and $\ddot{\beta}$ are as compared to the values from numerical differentiation. It was found that the $\hat{\beta}$ estimate from the Kalman filter is considerably less accurate than the filtered measurement data used in the Kalman filter. The $\hat{\beta}$ estimate should, therefore, be discarded and the smoothed measured data for β should be used in the identification algorithm of Eqs. (12) and (13) together with the Kalman filter estimates $\hat{\dot{\beta}}$, $\hat{\ddot{\beta}}$. Fig. 7 compares the estimate $\hat{\gamma}$ and associated variance from Fig. 3(a) with the values obtained with the Kalman filter for $\gamma = 4.2$ instead of 5.0. The large improvement by using $\hat{\dot{\beta}}$, $\hat{\ddot{\beta}}$ from the Kalman filter is evident. Fig. 7 suggests the possibility of an iteration procedure for the simultaneous estimation of state variables and parameters. The new value of $\hat{\gamma}$ could be used for an improved estimate of $\dot{\beta}$ and $\ddot{\beta}$ to be inserted once more into the identification algorithm of Eqs. (12) and (13). The errors of the smoothed measurements of β and additional modeling errors will remain, so that a true convergence of the iteration method cannot be expected. Nevertheless the results of one or two iterations would provide some clues as to the accuracy of the parameter estimate.

Estimation from Combined Transient and Trim Response

The separation of transient and trim response is not straight forward. One way of achieving such a separation is to Fourier analyze the pure trim response, compute the Fourier terms for the sample points used in analyzing the transient and subtract these Fourier terms from the combined transient and trim response. Small differences of large numbers may occur in this process and may cause errors in the result. In case of the pitch stirring model rotor another complication arises. The trim response cannot be measured while the eccentric which produces cyclic pitch stirring is installed. Only after replacing the eccentric by a pin without eccentricity, can the trim response be measured in a separate test run. In this case the separation of the transient and the trim response will involve errors from setting up identical test conditions in two different test runs. It was, therefore, believed to be of importance to look into the possibility of estimating γ directly from the combined transient and trim response.

The rotor control plane angle of attack for the planned transient model tests is nominally zero. Whatever actual small angle of attack may exist is considered by a correction of the collective pitch angle. We will thus assume, that the entire trim response is caused by an equivalent collective pitch angle which is not well known and which must be included in the parameter estimation.

For the computer experiments a step input of a collective pitch angle of 2 was performed at time zero, and the normal flow transient input, either in form of a rectangular or a wave shaped pulse was started at time 12. The identification was performed between time 12 and time 20. Fig. 8 shows the transient responses and the combined transient and trim responses for the two types of normal flow pulses. The two parameters to be identified with Eqs. (12) and (13) are γ and $\gamma\ \theta_o = \delta$. Figs. 9(a) and 9(b) show the estimates $\hat{\gamma}$ and $\hat{\delta}$ from the unpolluted combined trim and transient responses to the two types of normal flow pulses given in Figs. 1 and 2. The initial values for the covariance matrix were

$$P_o = \begin{bmatrix} P_{\gamma_o} = 2000 & 0 \\ 0 & P_{\delta_o} = 2800 \end{bmatrix}$$

It is seen that γ is identified with about the same accuracy as for the transients alone, Figs. 2(a) and 2(b), while δ is also identified with good accuracy.

The case of noise pollution with $\sigma_\beta = .1$ was also studied. The digital filter method with a cut-off frequency range of 2.5 to 2.9 resulted in very good estimates for $\hat{\gamma}$, both for the rectangular normal flow pulse and for the wave shaped pulse. The estimate for $\delta = \gamma\theta_o$ was 10% low in both cases. The filter cut-off frequency range of 2.5 - 2.9 probably was not optimal.

The method described in the preceding section was also applied to the two parameter estimation case, inserting into the Kalman filter equations values of $\gamma = 4.5$ instead of 5.0 and $\delta = 9.0$ instead of 10. Again the identification was performed with the noise polluted ($\sigma_\beta = .1$) digitally filtered (cut-off frequency 2.5 - 2.9) values for β and with the Kalman filter estimates for $\hat{\dot{\beta}}$ and $\hat{\ddot{\beta}}$. Figs. 10(a) and 10(b) show the results.

The method works very well also for the two parameter identification and provides an excellent estimate $\hat{\gamma}$ and somewhat reduced accuracy for $\hat{\delta}$. It may be possible to improve the latter by selecting a more favorable digital filter cut-off frequency.

Parameter Estimation from Multiblade Responses

When using multiblade flapping coordinates, see Reference [11], there exists the possibility to introduce two different equivalent blade Lock numbers, one for those aerodynamic terms which refer to rotor pitching and rolling moments, and a different one for the aerodynamic terms which refer to rotor thrust. It is intended to try this concept out in future rotor model tests. Here the results of some computer experiments are presented which are based on a multiblade coordinate representation, using however only a single value of the blade Lock number to be identified. The responses to the normal flow pulses shown in Fig. 1 were obtained from the complete equations including the periodic terms. They are shown in Fig. 11. For the identification a simplified system description has been used, see Reference [12] and Part I of this report, which omits periodic terms and the multiblade accelerations. As indicated in Fig. 11, only the rates of the multiblade coordinates β_o, β_I, β_{II} are used. Thus a modeling error is introduced into the identification algorithm.

Fig. 12 shows the results of the identification performed with Eqs. (12) and (13). The initial variance was P_o = 1000, the initial estimate $\hat{\gamma}(o)$ = 0. The error covariance matrix was assumed to be

$$R = \begin{bmatrix} 10 & 0 & 0 \\ 0 & 10 & \\ 0 & 0 & 10 \end{bmatrix}$$

Four cases are shown in Fig. 12.

1. The responses are unpolluted by noise. The identification for the wave shaped pulse, Fig. 12(b), is excellent. For the rectangular pulse, Fig. 12(a), there is a 7% bias error because the simplified model cannot follow the rapid changes in response, indicated in Fig. 11(a).
   As explained in Part I of this report the first order dynamics rotor representation is good for low frequencies but introduces increasing errors for increasing frequencies.

2. The unpolluted response is filtered with a digital filter with a cut-off frequency range of 1.7 - 1.9. The result of the identification from the rectangular pulse, Fig. 12(a), is greatly improved, resulting now in only 2% bias error. For the wave shaped pulse the identification is not much changed from the case without filter, since the wave input excites the higher frequencies of β to a lesser degree as is seen in Figs. 11(a) and 11(b).
3. Response deflections and their rates are polluted by zero mean computer generated Gaussian sequences with standard deviations indicated in Figs. 11(a) and (b). This results for the rectangular pulse in a large bias error of 18%, for the wave shaped pulse in a smaller bias error of 8%.
4. The noise polluted responses are filtered with the same filter as in case 2. Now the identification yields very accurate results for the wave shaped pulse, somewhat less accurate results for the rectangular pulse.

One can conclude from these experiments that filtering of the responses with a digital filter with cut-off frequency range of 1.7 - 1.9 not only removes much of the bias error from the noise pollution, but it also removes the modeling bias error. It was found that filtering with a cut-off frequency range of .6 - .9 gave poor γ identification, particularly in the rectangular pulse case. Using a smoother pulse shape with less high frequency contents and increasing the filter cut-off frequency range ot 1.7 - 1.9 resulted in very accurate identification in spite of the simplified analytical model.

As mentioned before, only deflections will be measured in the transient rotor model tests. A further set of computer experiments assumed, therefore, that only β_o, β_I, β_{II} are available and pulluted by noise with a standard deviation indicated in Fig. 11. The deflections were filtered with a cut-off frequency range of 1.7 - 1.9 and numerically differentiated to obtain $\dot{\beta}_o$, $\dot{\beta}_I$, $\dot{\beta}_{II}$. The identification result is shown in Fig. 13. The identification of $\hat{\gamma}$ is excellent for the wave shaped pulse, less good for the rectangular pulse. Probably the latter case could be improved in a similar way as was shown for the single blade by applying a Kalman filter with the estimated γ to obtain $\hat{\dot{\beta}}_o$, $\hat{\dot{\beta}}_I$, $\hat{\dot{\beta}}_{II}$ rather than applying numerical differentiation.

Conclusion

The computer experiments were performed with a simple linear parameter identification algorithm. The estimation of blade Lock number and collective pitch angle was based on the availability of noise polluted blade flapping measurements without knowing the flapping rates or accelerations. It was found that the linear estimator worked very well provided the data were properly processed by applying a digital filter with an optimal cut-off frequency between 2 and 3. The filter removed much of the bias in the estimate caused by the noise pollution, and it also removed most of the bias in the multiblade estimate from modeling errors incurred by omitting periodic terms and multiblade flapping accelerations. Substantial improvement of the estimates were possible if the numerical differentiation of the polluted filtered flapping deflection was replaced by Kalman filtering with the system equations using first estimates for the parameters. A continuation of the computer experiments is planned to encompass more complex situations of rotor parameter identification.

References

1. Chen, R. T. N., Eulrich, B. J. and Lebacqz, J. V., Development of Advanced Techniques for the Identification of V/STOL Aircraft Stability and Control Parameters", Cornell Aeronautical Laboratory Report. No. BM-2820-F-1, August 1971.
2. Molusis, J. A., "Helicopter Stability Derivative Extraction from Flight Data Using the Bayesian Approach to Estimation", Journal of the American Helicopter Society, Vol. 18, No. 2, April 1973, pp. 12-23.
3. Hohenemser, K. H. and Prelewicz, D. A., "Computer Experiments on Periodic Systems Identification Using Rotor Blade Transient Flapping-Torsion Responses at High Advance Ratio". Proceedings Specialists Meeting on Rotorcraft Dynamics, AHS/NASA/Ames, Moffett Field, California, February 1974.
4. Kuczynski, W. A., "Experimental Hingeless Rotor Characteristics at Full Scale First Flap Mode Frequencies", Lockheed Report LR 25491, October 1972.
5. Peters, D. A., "Hingeless Rotor Frequency Response with Unsteady Inflow", Proceedings Specialists Meeting on Rotorcraft Dynamics, AHS/NASA/Ames, Moffett Field, California, February 1974.

6. Ormiston, R. A. and Peters, D. A., "Hingeless Rotor Response with Non-Uniform Inflow and Elastic Blade Bending", Journal of Aircraft, Vol. 9, No. 10, October 1972, pp. 730 - 736.

7. Molusis, J. A., "Helicopter Stability Derivative Extraction and Data Processing Using Kalman Filtering Techniques", 28th Annual National Forum American Helicopter Society, Washington D.C., May 1972, Preprint 641.

8. Mehra, R. K., "Identification of Stochastic Linear Dynamic Systems Using Kalman Filter Representation", AIAA Journal, Vol. 9, No. 1, January 1971, pp. 28-31.

9. Bryson, A. E. and Ho, Y. C., "Applied Optimal Control", Ginn & Co., Waltham, Mass., 1969.

10. Graham, R. J., "Determination and Analysis of Numerical Smoothing Weights", NASA TR R-179, December 1963.

11. Hohenemser, K. H. and Yin, S. K., "Some Applications of the Method of Multiblade Coordinates", Journal American Helicopter Society, Vol. 17, No. 3, July 1972.

12. Hohenemser, K. H. and Yin, S. K., "On the Use of First Order Rotor Dynamics in Multiblade Coordinates", 30th Annual National Forum American Helicopter Society, Washington D.C., May 1974, Preprint 831.

Figure Captions

Fig. 1 Normal Flow Pulse and Associated Flapping Response for $\mu = .4$, $\gamma = 5$, $\omega_1 = 1.2$

(a) Rectangular Pulse

(b) Wave Shaped Pulse

Fig. 2 Estimate $\hat{\gamma}$ and Associated Variance P/P_o for Unpolluted Responses

(a) Rectangular Pulse

(b) Wave Shaped Pulse

Fig. 3 Estimate $\hat{\gamma}$ and Associated Variance for Polluted (σ_β = .2 and .05) Filtered (1.7 - 1.9) Responses.

(a) Rectangular Pulse

(b) Wave Shaped Pulse

Fig. 4 Ra*es of Flapping Deflection $\dot{\beta}$ for σ_β = 0 and .2 from Numerically Differentiating Filtered Response β.

(a) Rectangular Pulse

(b) Wave Shaped Pulse

Fig. 5 Diagonal Terms of Covariance Matrix for Kalman Filter, Rectangular Pulse.

Fig. 6 Flapping Rates and Accelerations. Exact Values (σ_β = 0), from Numerically Differentiating filtered Response β (σ_β = .2), and from Kalman Filter with γ = 4.2.

Fig. 7 Estimates $\hat{\gamma}$ and Associated Variance P/P_o for σ_β = .2, Digital Filter and Kalman Filter for γ = 4.2 Rectangular Pulse.

Fig. 8 Transient Response and Combined Transient and Trim Response for θ_o = 2.

(a) Rectangular Pulse

(b) Wave Shaped Pulse

Fig. 9 — Estimates $\hat{\gamma}$ and $\hat{\delta}$ and Diagonal Components of Associated Covariance Matrix from Unpolluted Responses with $\theta_o = 2$

(a) Rectangular Pulse

(b) Wave Shaped Pulse

Fig. 10 — Estimates $\hat{\gamma}$ and $\hat{\delta}$ and Diagonal Components of Associated Covariance Matrix for Polluted ($\sigma_\beta = .1$), Filtered (2.5 - 2.9) Responses Using Kalman Filter with $\gamma = 4.5$ and $\delta = 9$.

(a) Rectangular Pulse

(b) Wave Shaped Pulse

Fig. 11 — Normal Flow Pulse and Associated Multiblade Flapping Responses for $\mu = .4$, $\gamma = 5$, $\omega_1 = 1.2$

(a) Rectangular Pulse

(b) Wave Shaped Pulse

Fig. 12 — Estimate $\hat{\gamma}$ and Associated Variance P for Unpolluted, Unpolluted Filtered (1.7 - 1.9), Polluted, and Polluted Filtered Multiblade Responses, β_o, β_I, β_{II}, $\dot{\beta}_o$, $\dot{\beta}_I$, $\dot{\beta}_{II}$ given.

(a) Rectangular Pulse

(b) Wave Shaped Pulse

Fig. 13 — Estimate $\hat{\gamma}$ and Associated Variance P for Polluted, Filtered (1.7 - 1.9), Differentiated Multiblade Responses, β_o, β_I, β_{II} given.

(a) Rectangular Pulse

(b) Wave Shaped Pulse

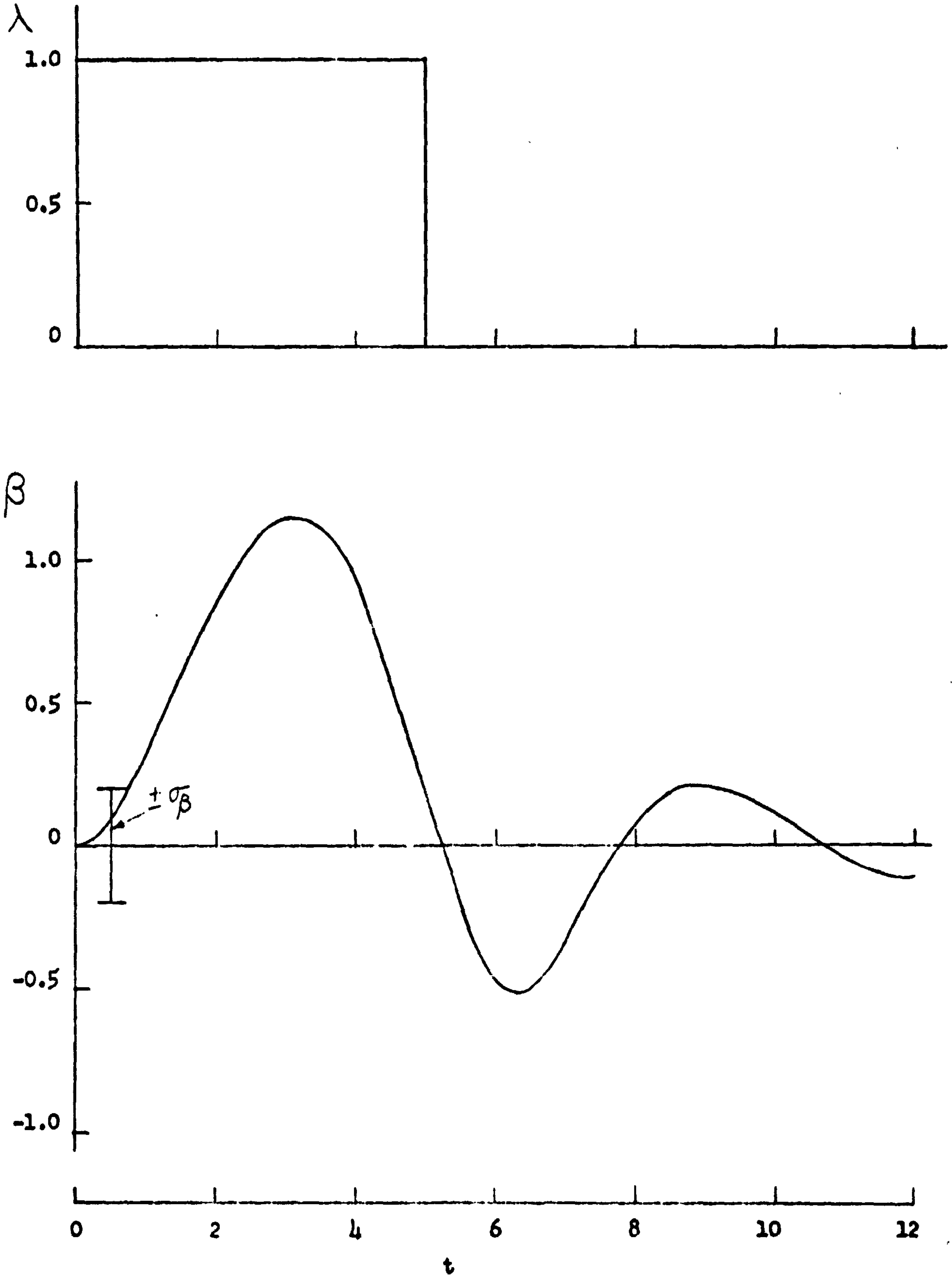

Fig. 1 (a)

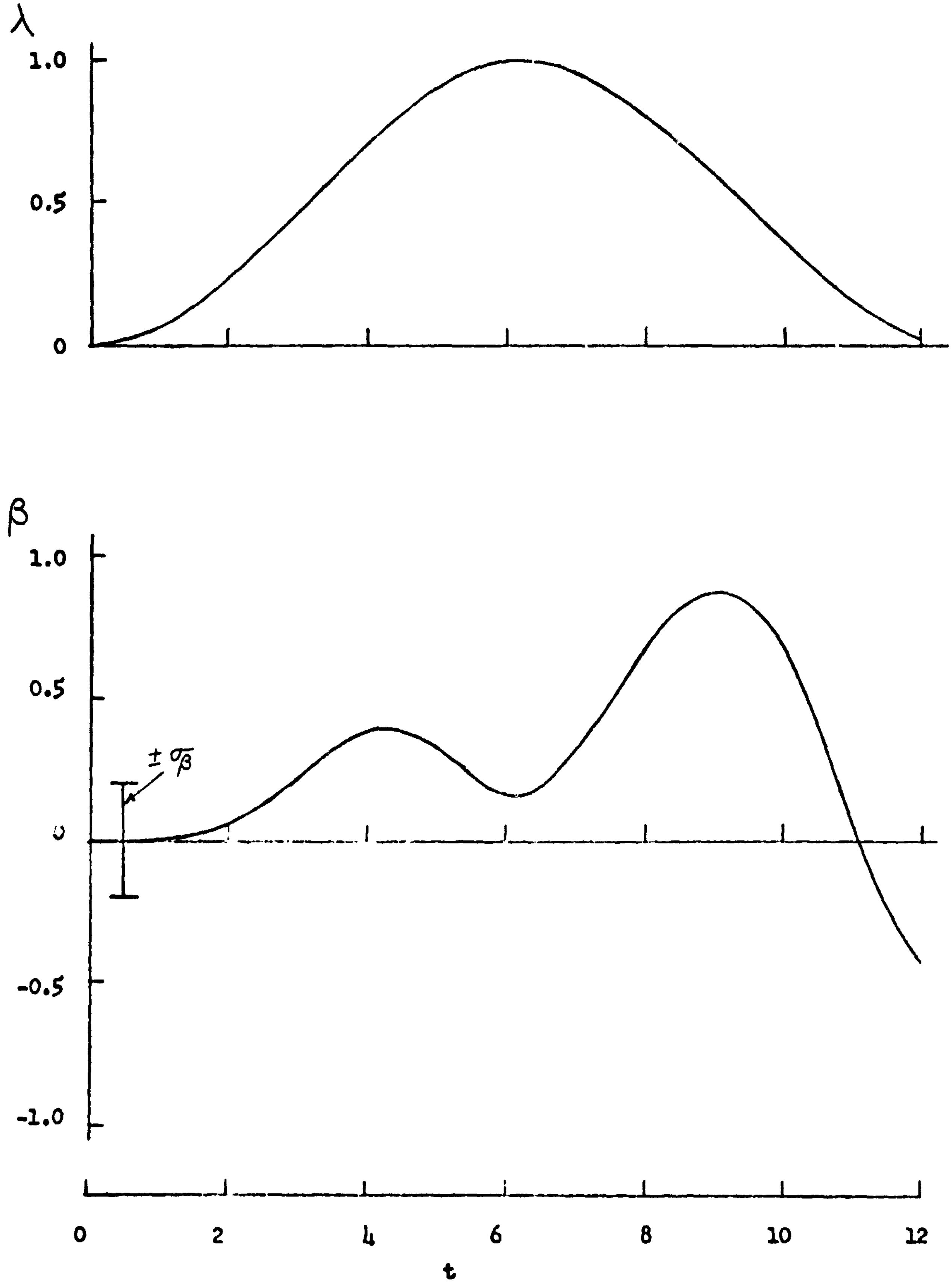

Fig. 1 (b)

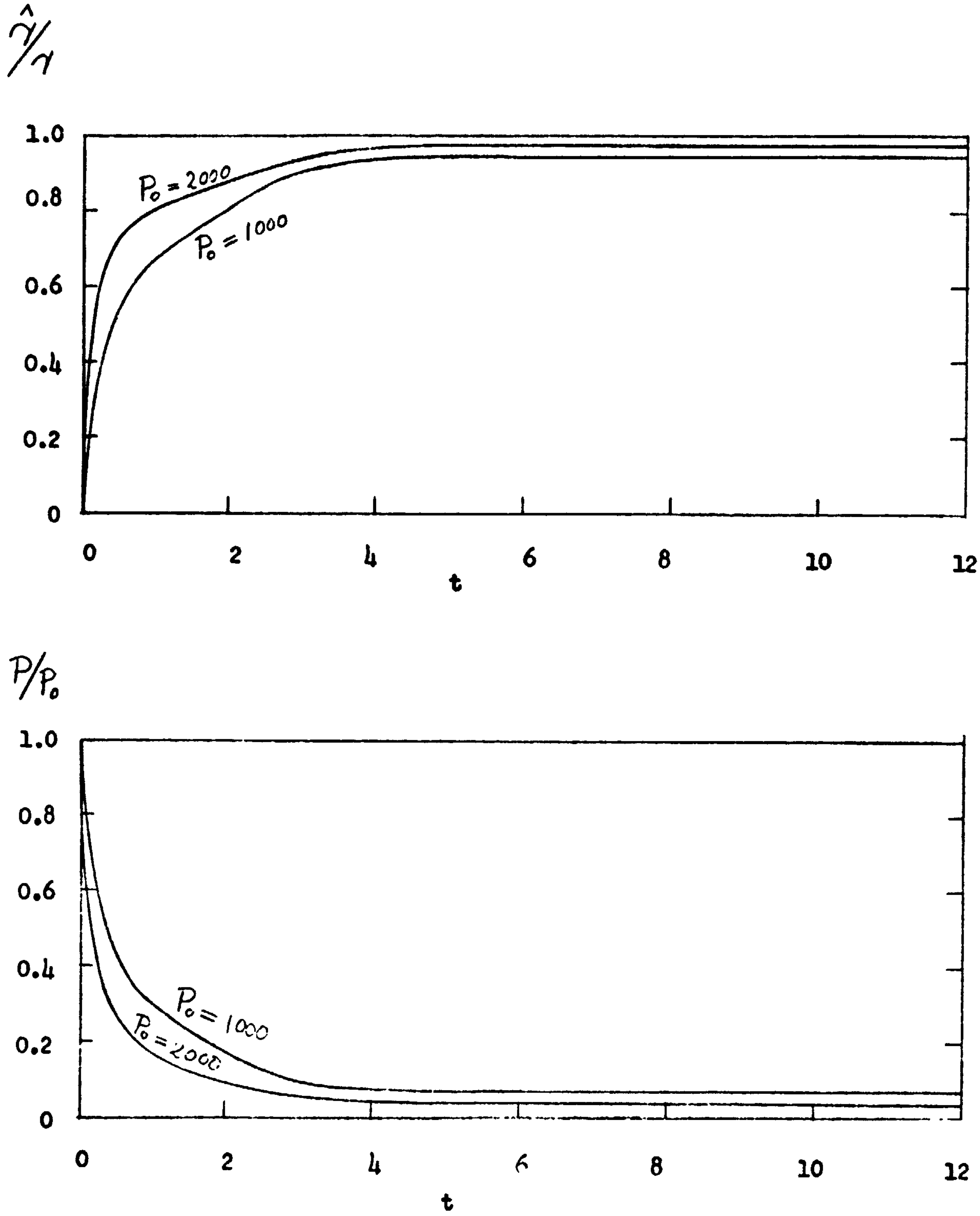
$\hat{\lambda}/\lambda$
1.0
0.8
0.6
0.4
0.2
0
$P_o = 2000$
$P_o = 1000$
0
2
4
6
8
10
12
t
P/P_o
1.0
0.8
0.6
0.4
0.2
0
$P_o = 1000$
$P_o = 2000$
0
2
4
6
8
10
12
t

Fig. 2 (a)

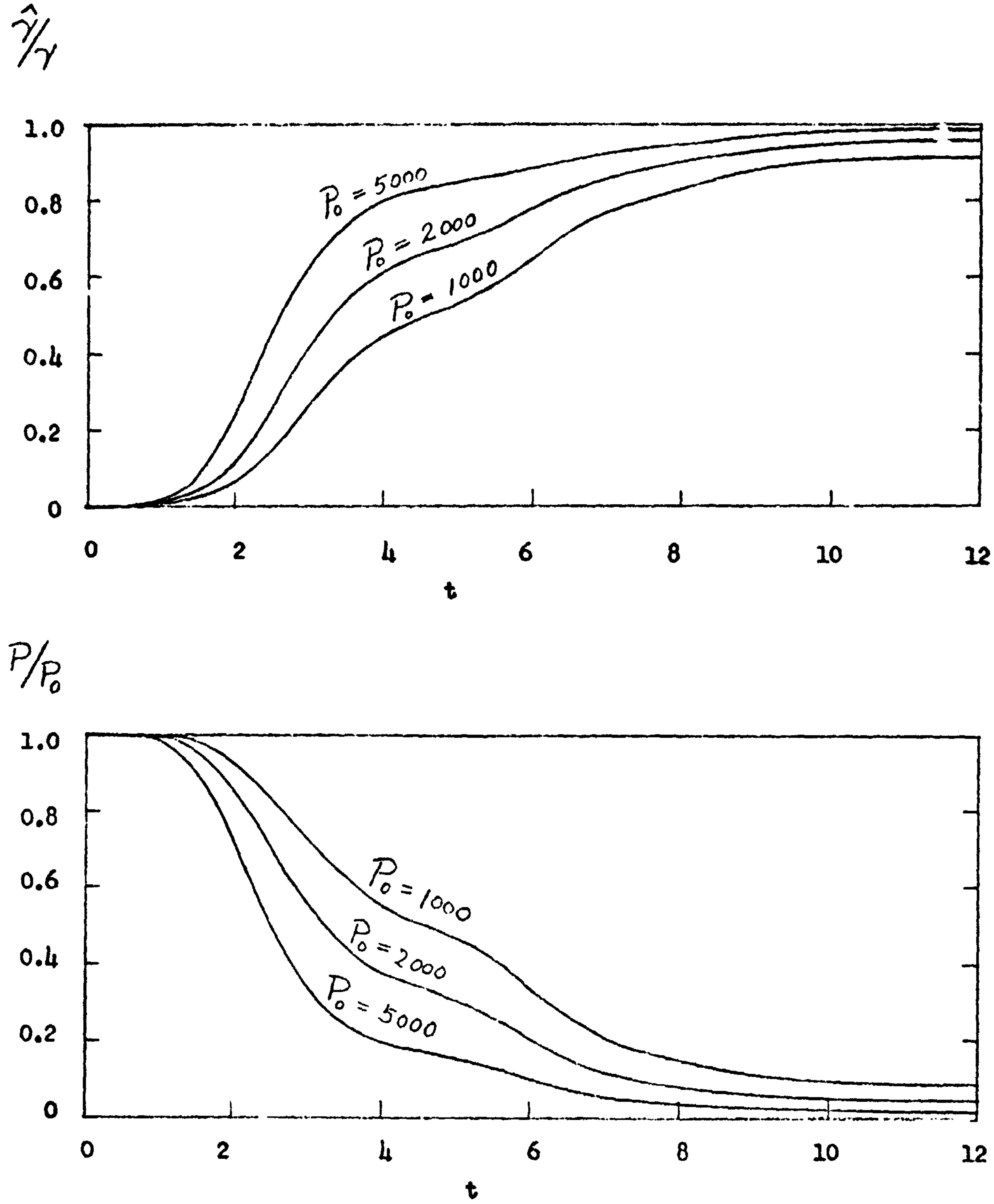

$\hat{\gamma}/\gamma$
1.0
0.8
0.6
0.4
0.2
0
$P_0 = 5000$
$P_0 = 2000$
$P_0 = 1000$
0
2
4
6
8
10
12
t
P/P_0
1.0
0.8
0.6
0.4
0.2
0
$P_0 = 1000$
$P_0 = 2000$
$P_0 = 5000$
0
2
4
6
8
10
12
t

Fig. 2 (b)

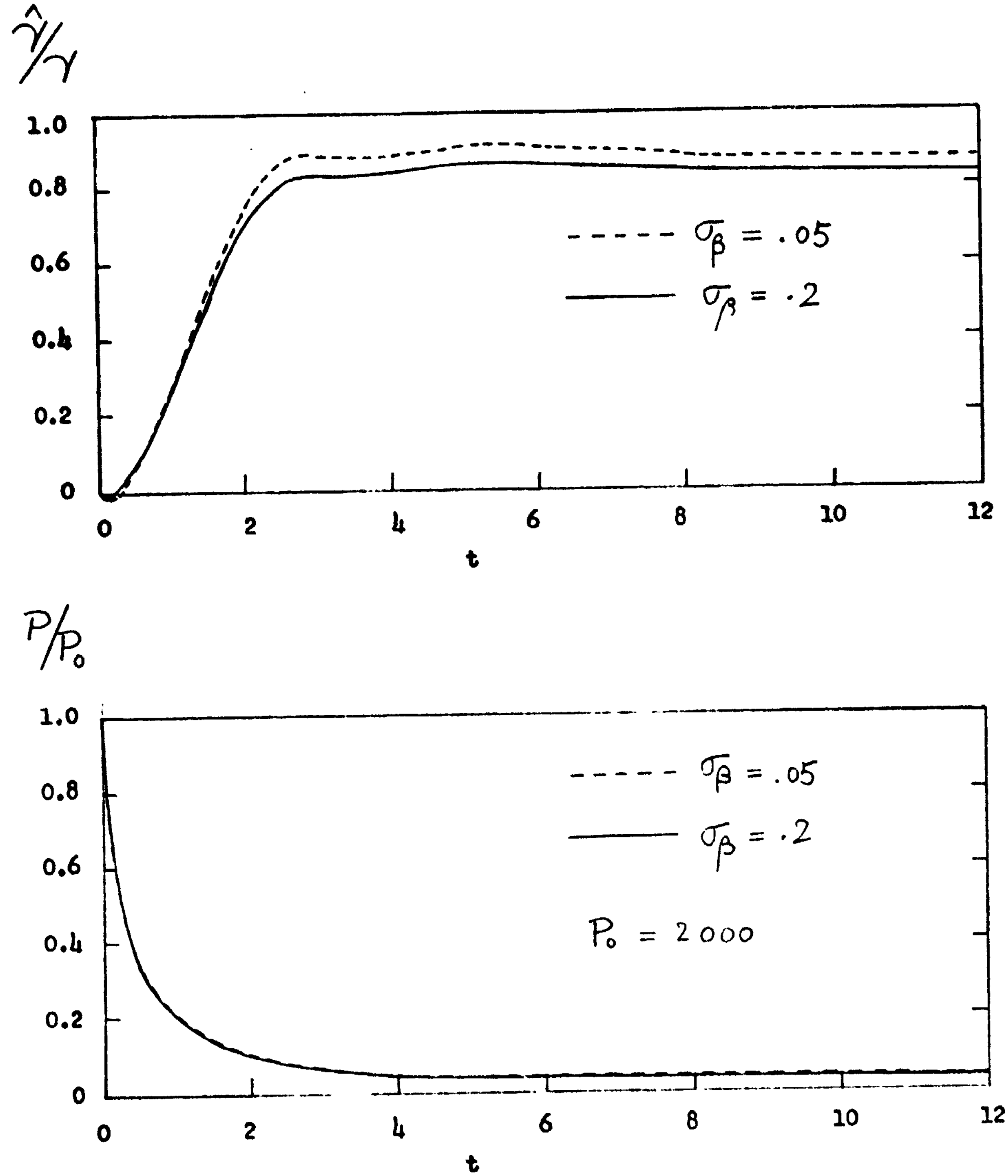

$\hat{\gamma}/\gamma$
1.0
0.8
0.6
0.4
0.2
0
0
2
4
6
8
10
12
t
$\sigma_\beta = .05$
$\sigma_\beta = .2$
P/P_o
1.0
0.8
0.6
0.4
0.2
0
0
2
4
6
8
10
12
t
$\sigma_\beta = .05$
$\sigma_\beta = .2$
$P_o = 2000$

Fig. 3 (a)

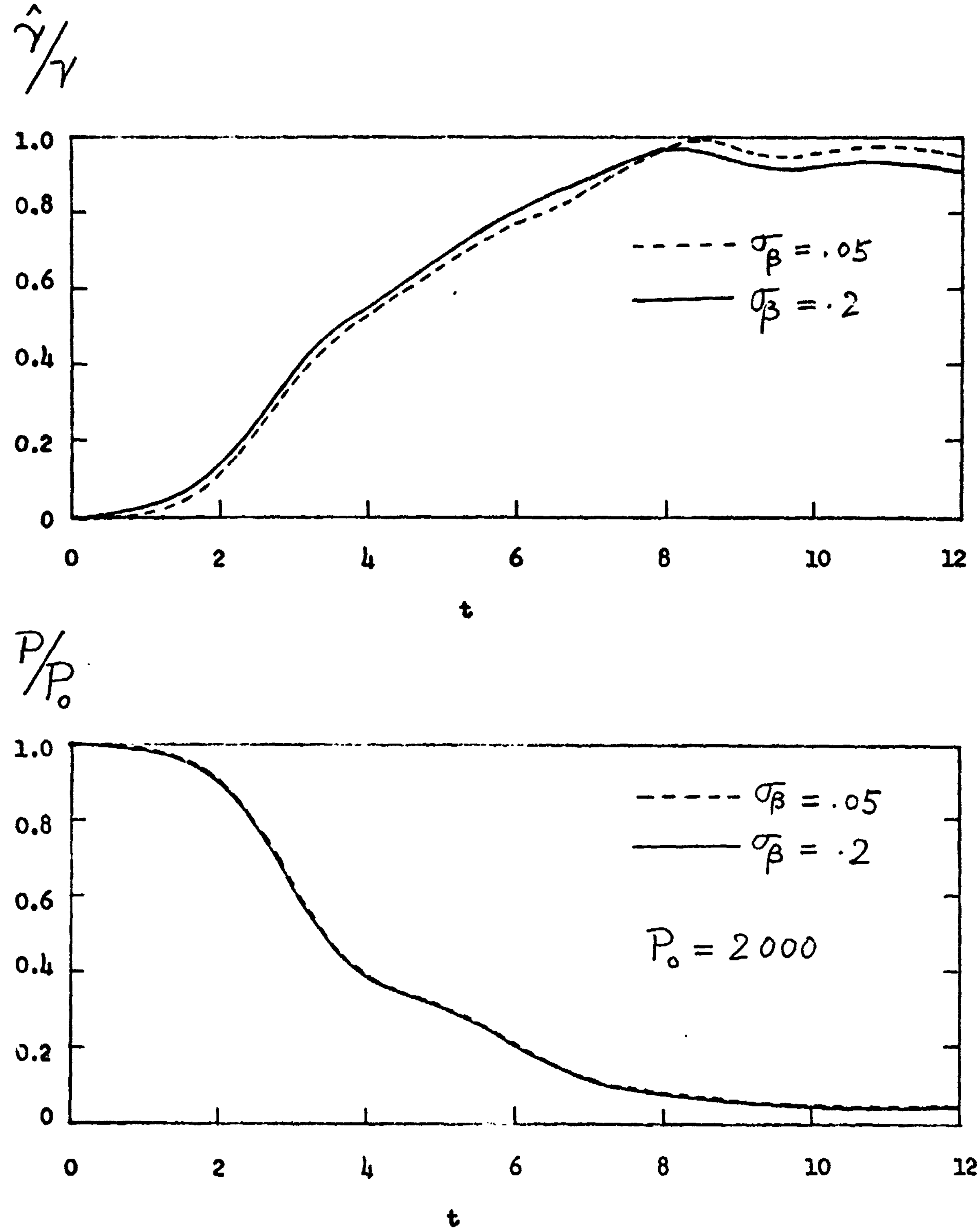

$\hat{\gamma}/\gamma$
1.0
0.8
0.6
0.4
0.2
0
0
2
4
6
8
10
12
t
$\sigma_\beta = .05$
$\sigma_\beta = .2$
P/P_o
1.0
0.8
0.6
0.4
0.2
0
0
2
4
6
8
10
12
t
$\sigma_\beta = .05$
$\sigma_\beta = .2$
$P_o = 2000$

Fig. 3 (b)

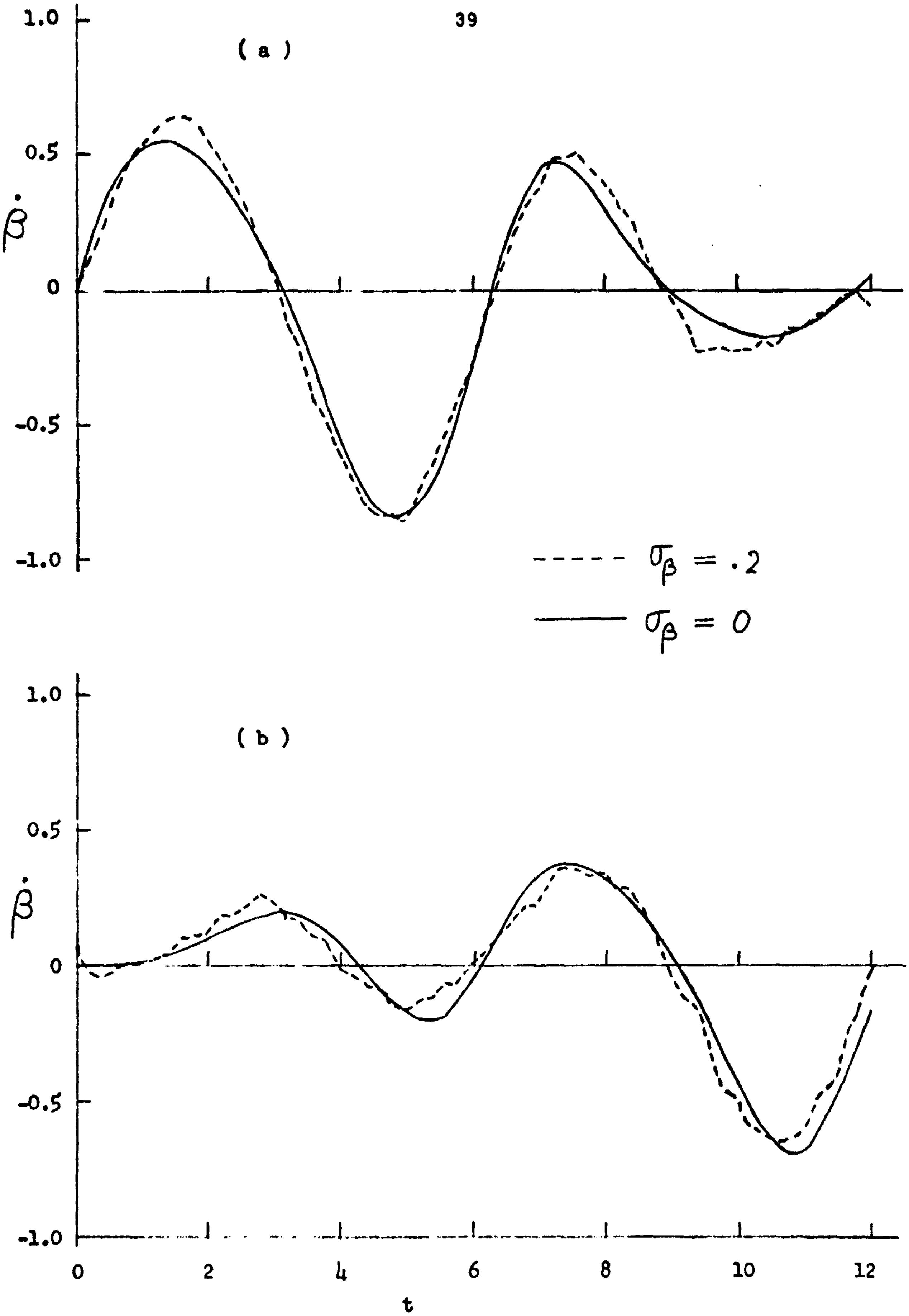
1.0
(a)
0.5
$\dot{\beta}$
0
-0.5
-1.0
$\sigma_\beta = .2$
$\sigma_\beta = 0$
1.0
(b)
0.5
$\dot{\beta}$
0
-0.5
-1.0
0
2
4
6
8
10
12
t

Fig. 4

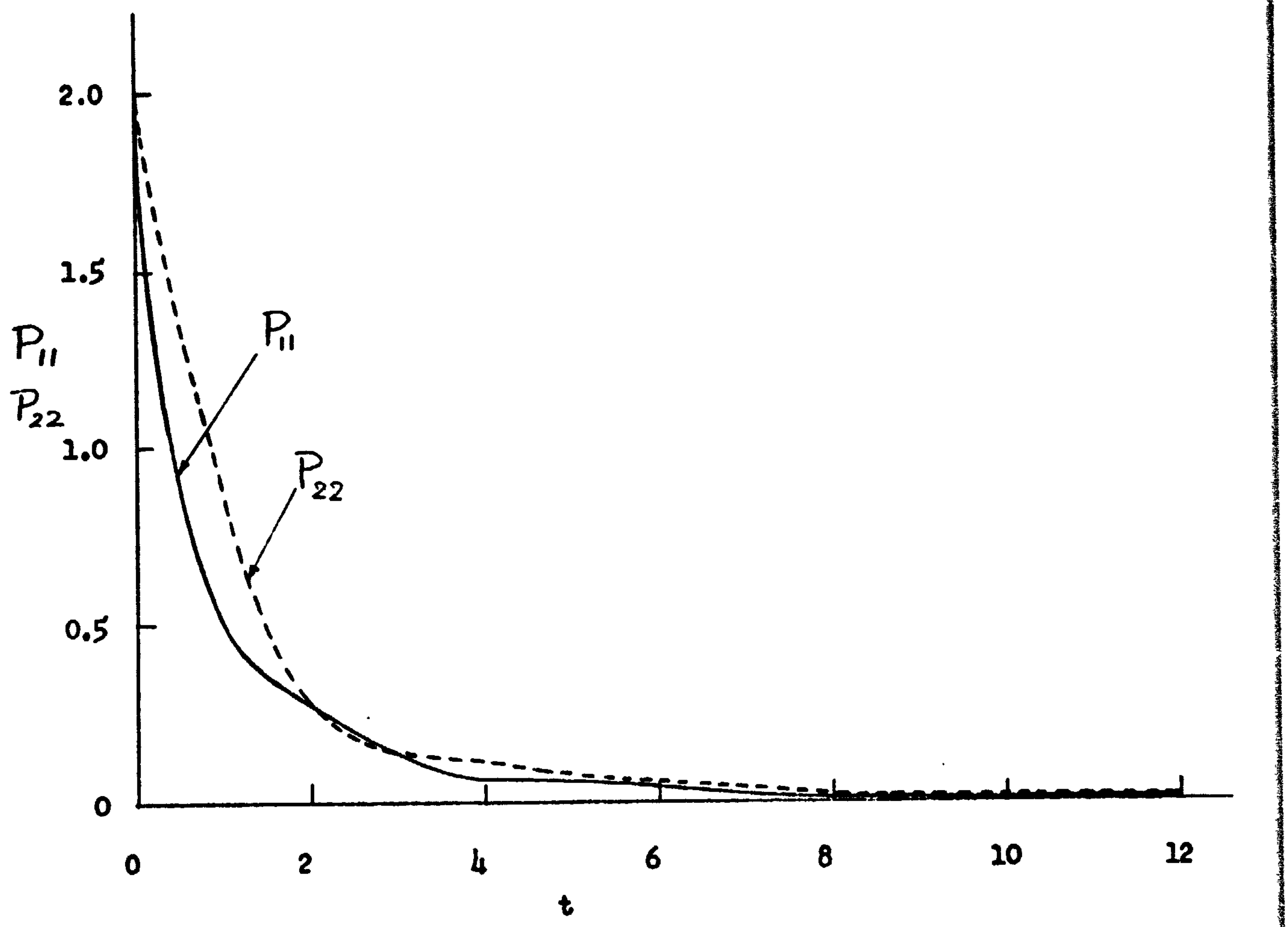

Fig. 5

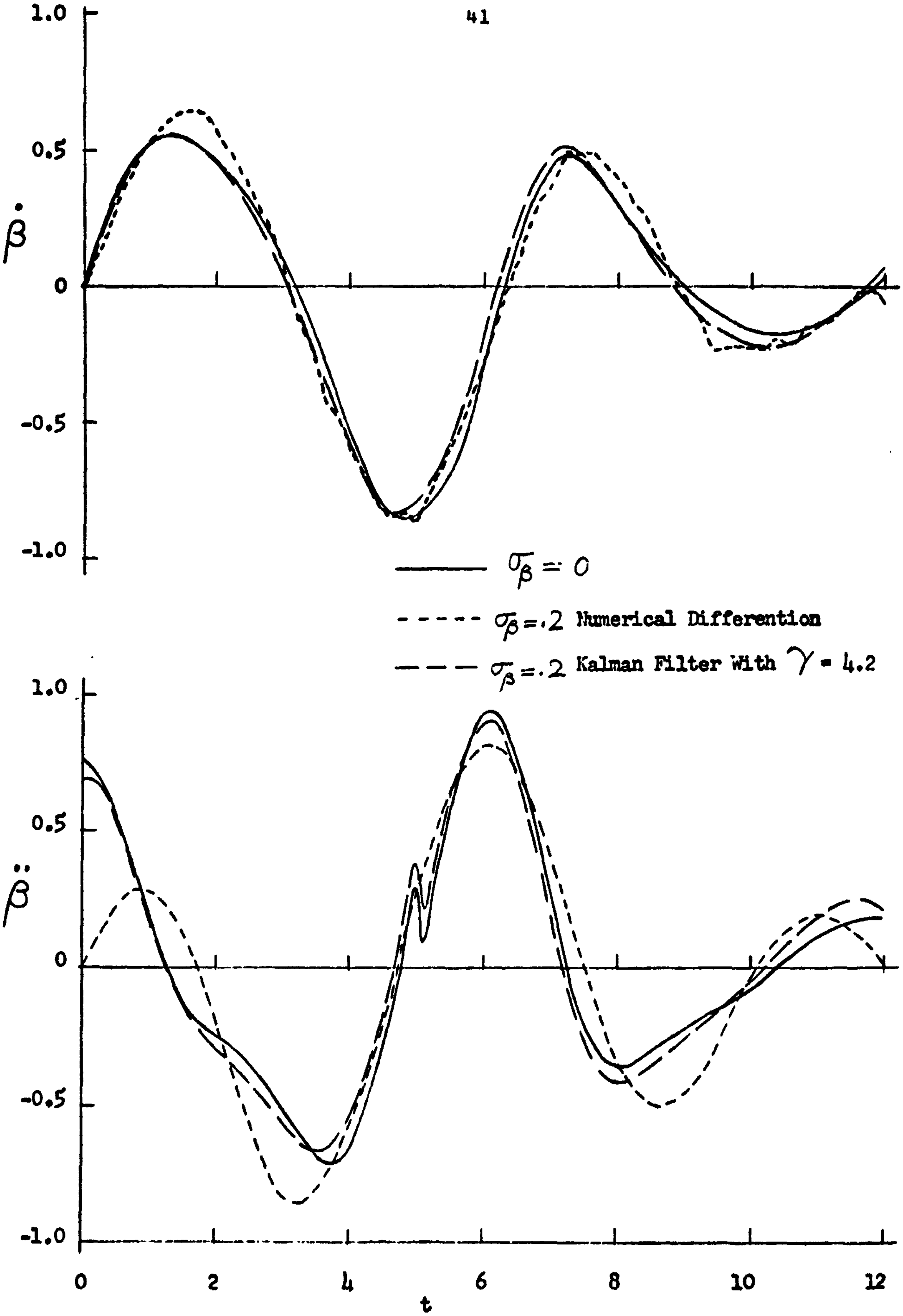
1.0
0.5
0
-0.5
-1.0
$\dot{\beta}$
$\sigma_\beta = 0$
$\sigma_\beta = .2$ Numerical Differention
$\sigma_\beta = .2$ Kalman Filter With $\gamma = 4.2$
1.0
0.5
0
-0.5
-1.0
$\ddot{\beta}$
0
2
4
6
8
10
12
t

Fig. 6

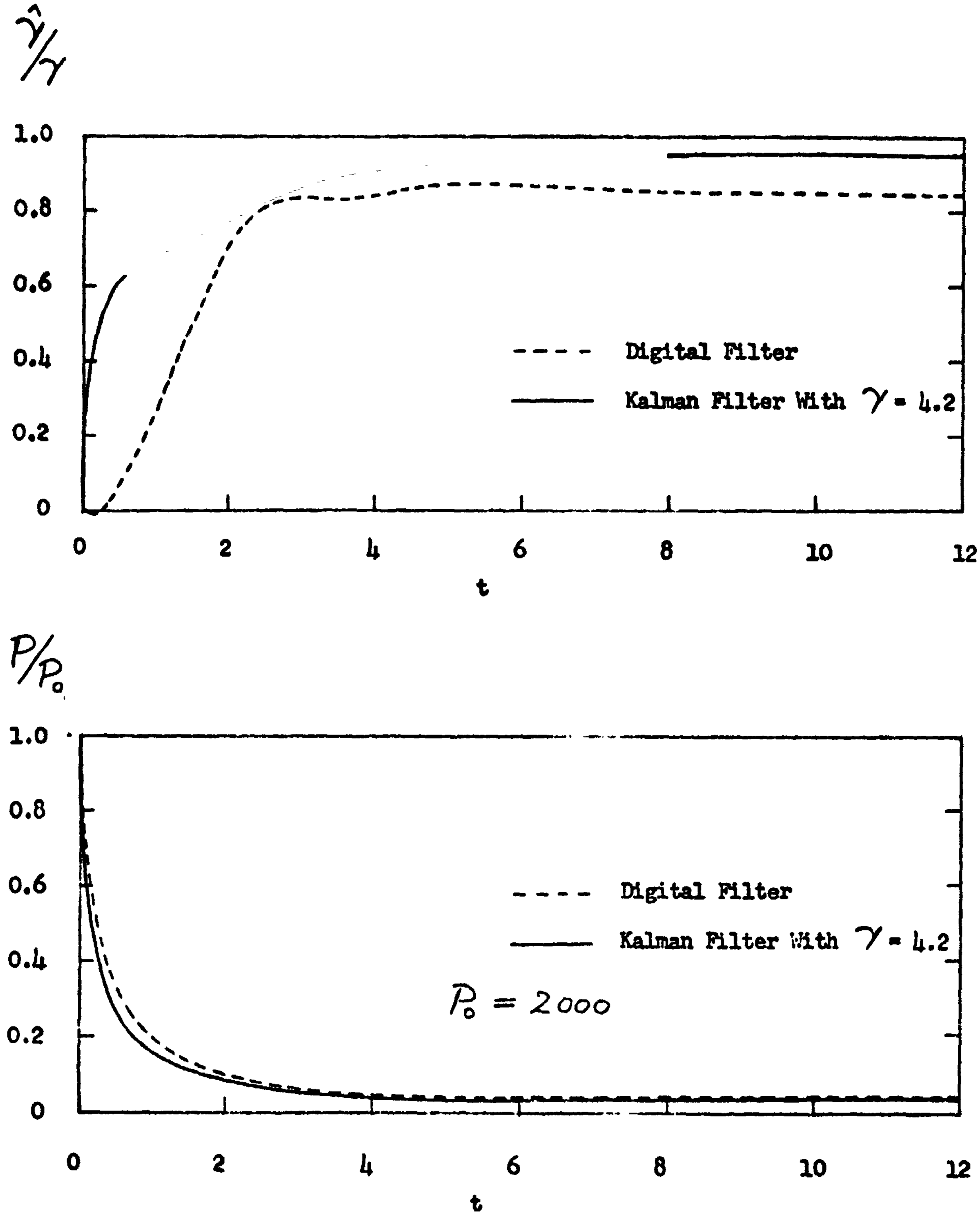

$\hat{\gamma}/\gamma$
1.0
0.8
0.6
0.4
0.2
0
0
2
4
6
8
10
12
t
Digital Filter
Kalman Filter With $\gamma = 4.2$
P/P_o
1.0
0.8
0.6
0.4
0.2
0
0
2
4
6
8
10
12
t
Digital Filter
Kalman Filter With $\gamma = 4.2$
$P_o = 2000$

Fig. 7

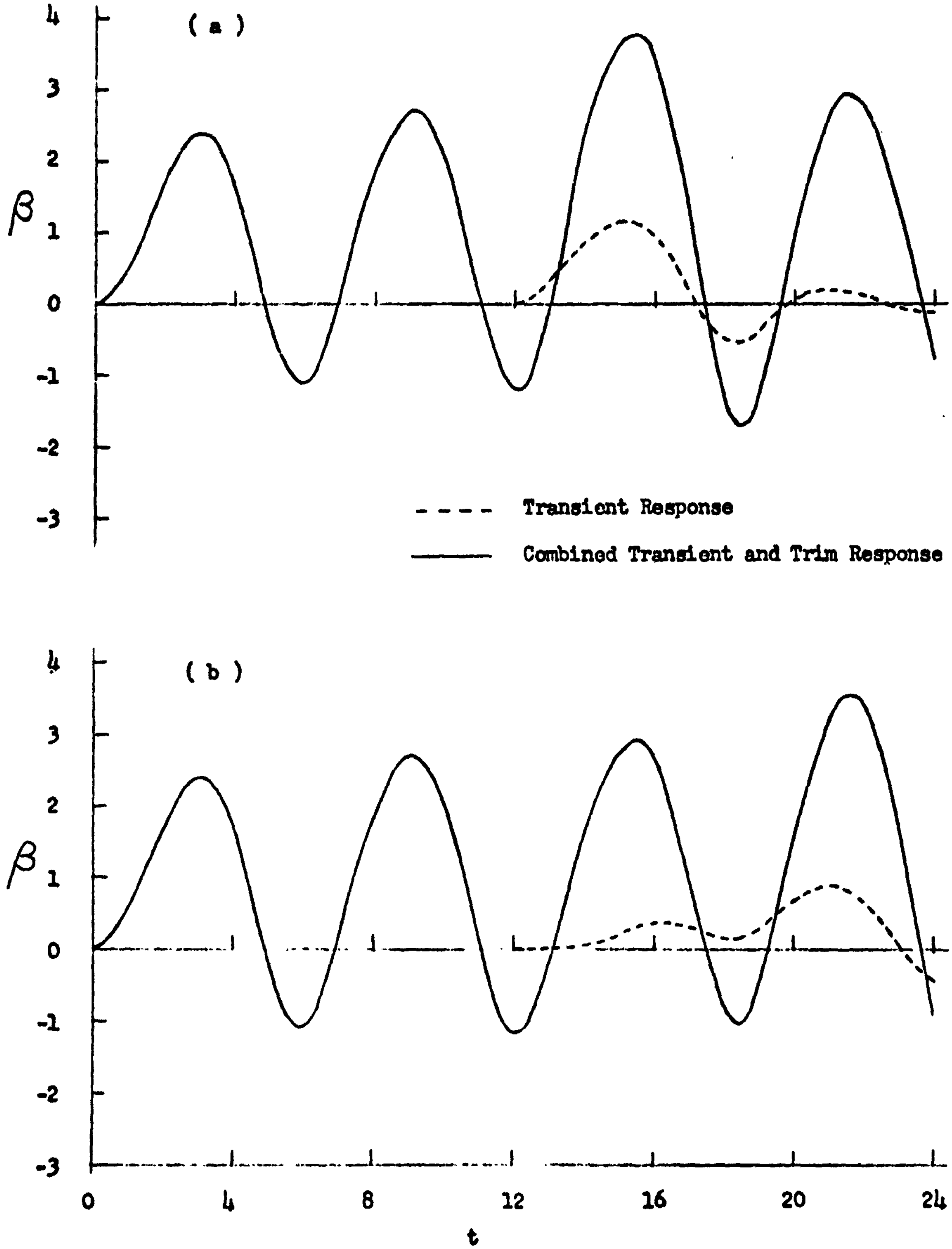
(a)
Transient Response
Combined Transient and Trim Response
(b)
β
t
0
4
8
12
16
20
24
-3
-2
-1
1
2
3

Fig. 8

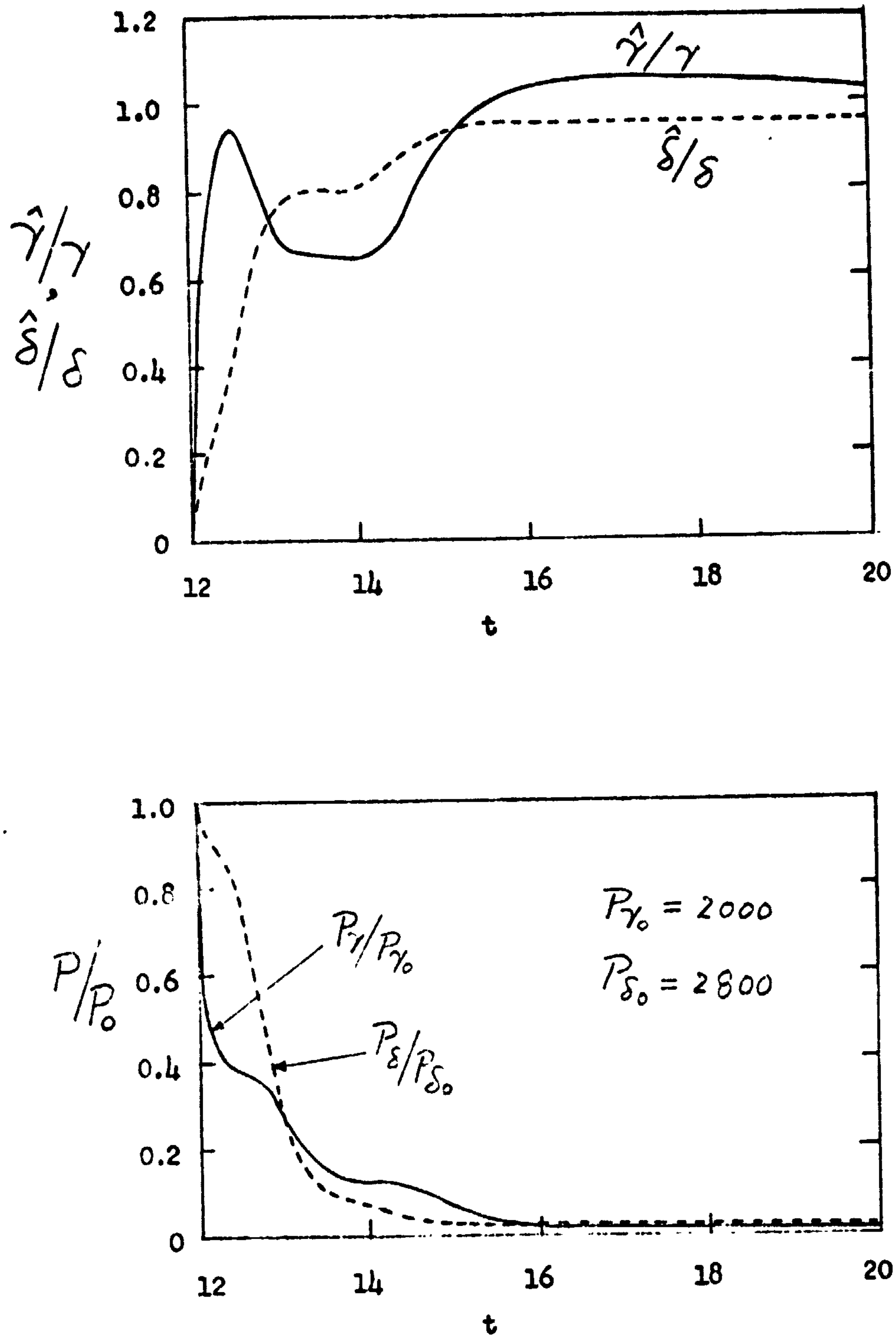
1.2
1.0
0.8
0.6
0.4
0.2
0
$\hat{\gamma}/\gamma$
$\hat{\delta}/\delta$
$\hat{\gamma}/\gamma$, $\hat{\delta}/\delta$
12
14
16
18
20
t
1.0
0.8
0.6
0.4
0.2
0
P/P_o
P_γ/P_{γ_o}
P_δ/P_{δ_o}
$P_{\gamma_o} = 2000$
$P_{\delta_o} = 2800$
12
14
16
18
20
t

Fig. 9 (a)

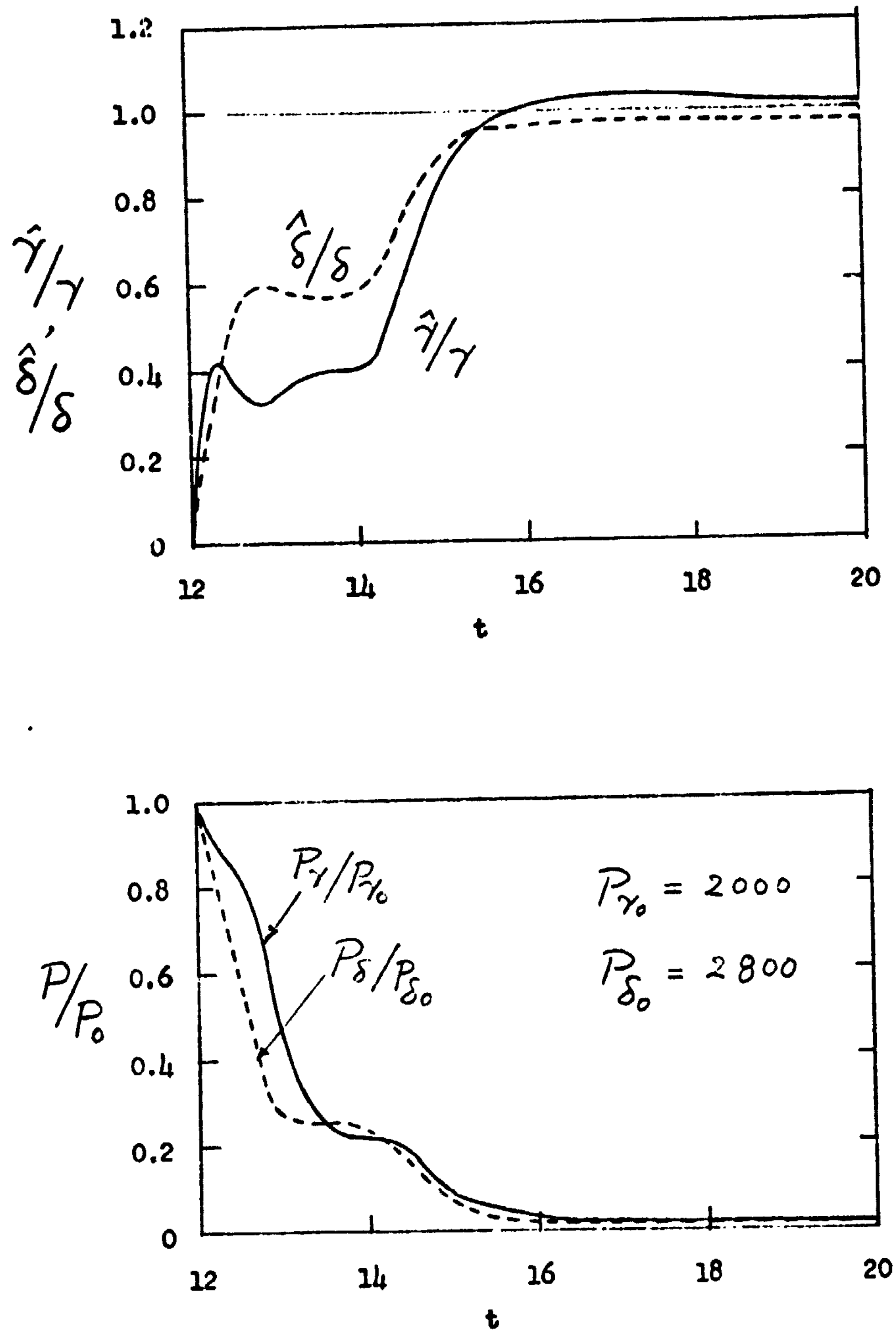

1.2
1.0
0.8
0.6
0.4
0.2
0
$\hat{\gamma}/\gamma$, $\hat{\delta}/\delta$
$\hat{\delta}/\delta$
$\hat{\gamma}/\gamma$
12
14
16
18
20
t
1.0
0.8
0.6
0.4
0.2
0
P/P_0
P_γ/P_{γ_0}
P_δ/P_{δ_0}
$P_{\gamma_0} = 2000$
$P_{\delta_0} = 2800$
12
14
16
18
20
t

Fig. 9 (b)

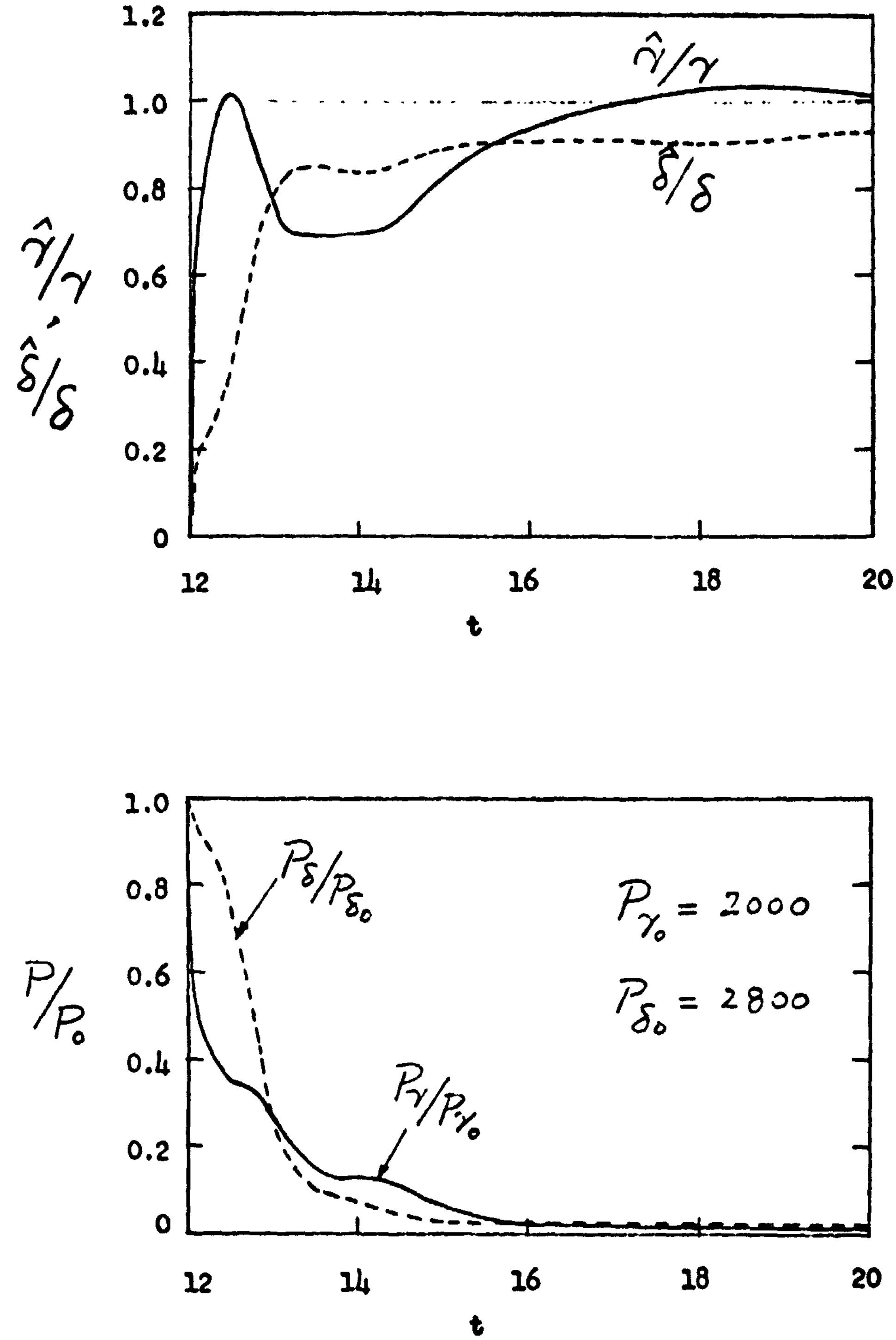
1.2
1.0
0.8
0.6
0.4
0.2
0
12
14
16
18
20
t
$\hat{\gamma}/\gamma$
$\hat{\delta}/\delta$
$\hat{\gamma}/\gamma$, $\hat{\delta}/\delta$
1.0
0.8
0.6
0.4
0.2
0
12
14
16
18
20
t
P/P_0
P_δ/P_{δ_0}
P_γ/P_{γ_0}
$P_{\gamma_0} = 2000$
$P_{\delta_0} = 2800$

Fig. 10 (a)

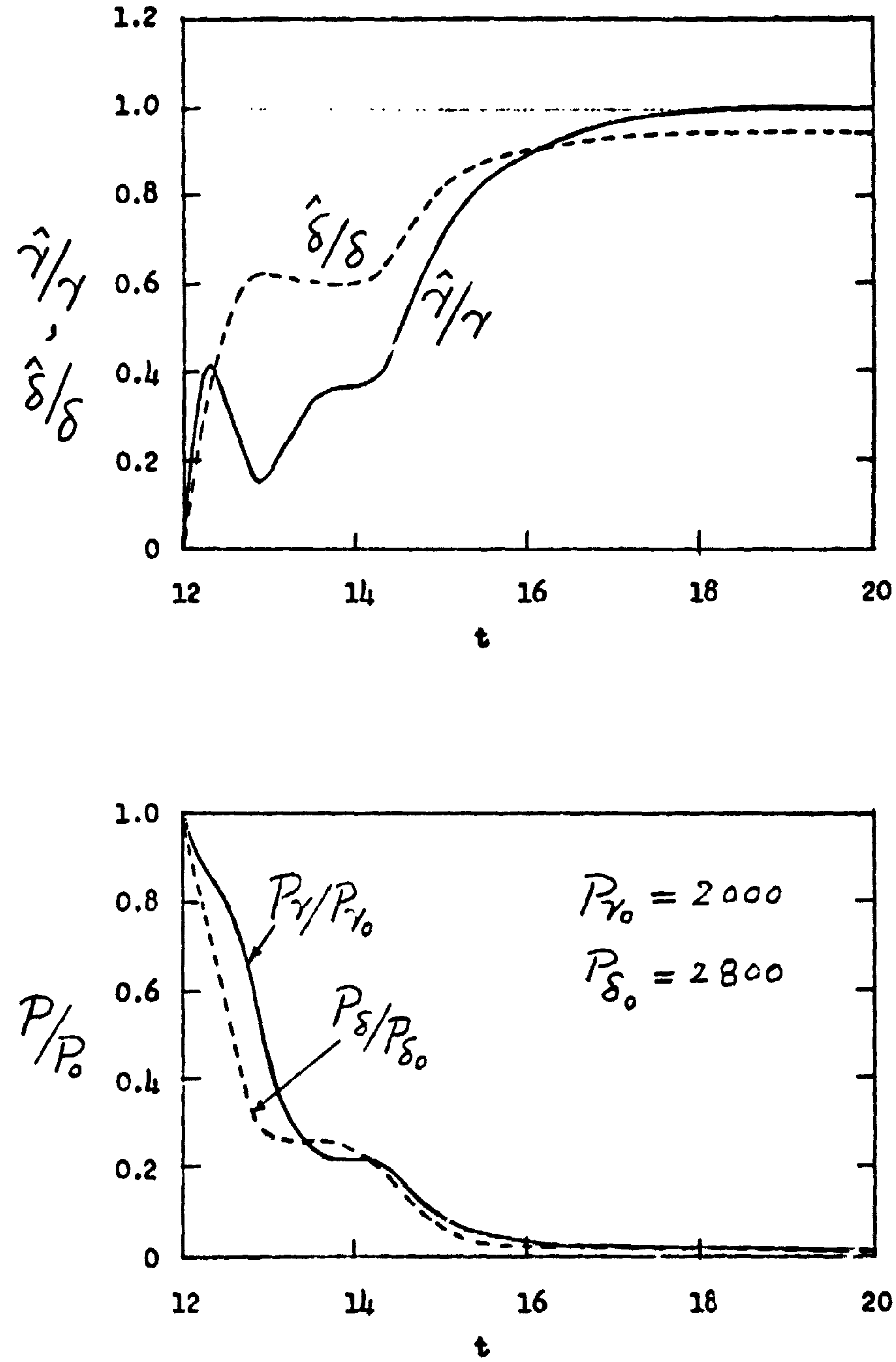
1.2
1.0
0.8
0.6
0.4
0.2
0
12
14
16
18
20
t
$\hat{\gamma}/\gamma$, $\hat{\delta}/\delta$
$\hat{\delta}/\delta$
$\hat{\gamma}/\gamma$
1.0
0.8
0.6
0.4
0.2
0
12
14
16
18
20
t
P/P_0
P_γ/P_{γ_0}
P_δ/P_{δ_0}
$P_{\gamma_0} = 2000$
$P_{\delta_0} = 2800$

Fig. 10 (b)

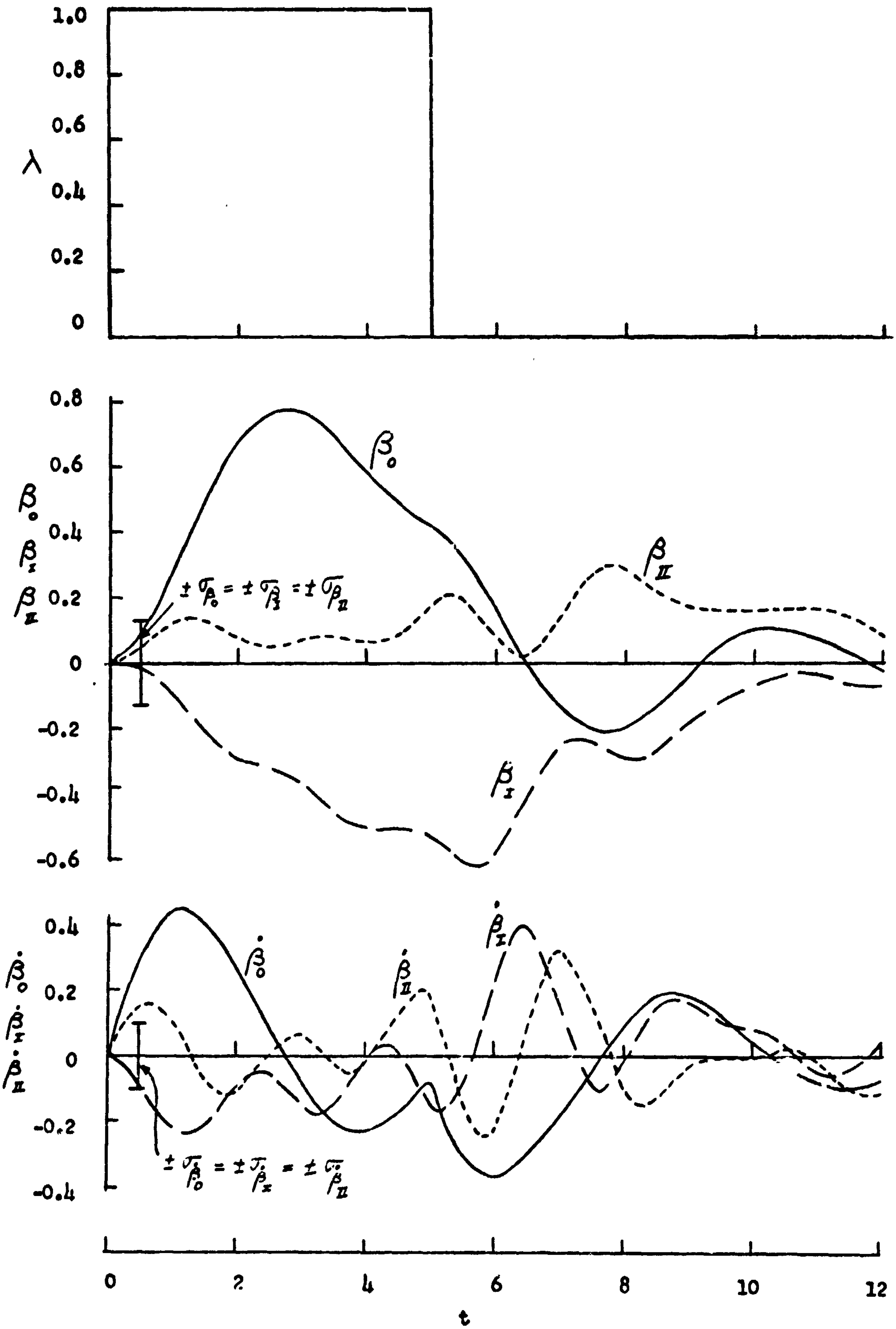
1.0
0.8
0.6
λ
0.4
0.2
0
0.8
0.6
β_0
0.4
β_I
β_{II}
0.2
0
-0.2
-0.4
-0.6
$\pm\sigma_{\beta_0} = \pm\sigma_{\beta_I} = \pm\sigma_{\beta_{II}}$
0.4
$\dot\beta_0$
0.2
$\dot\beta_I$
$\dot\beta_{II}$
0
-0.2
-0.4
$\pm\sigma_{\dot\beta_0} = \pm\sigma_{\dot\beta_I} = \pm\sigma_{\dot\beta_{II}}$
0
2
4
6
8
10
12
t

Fig. 11 (a)

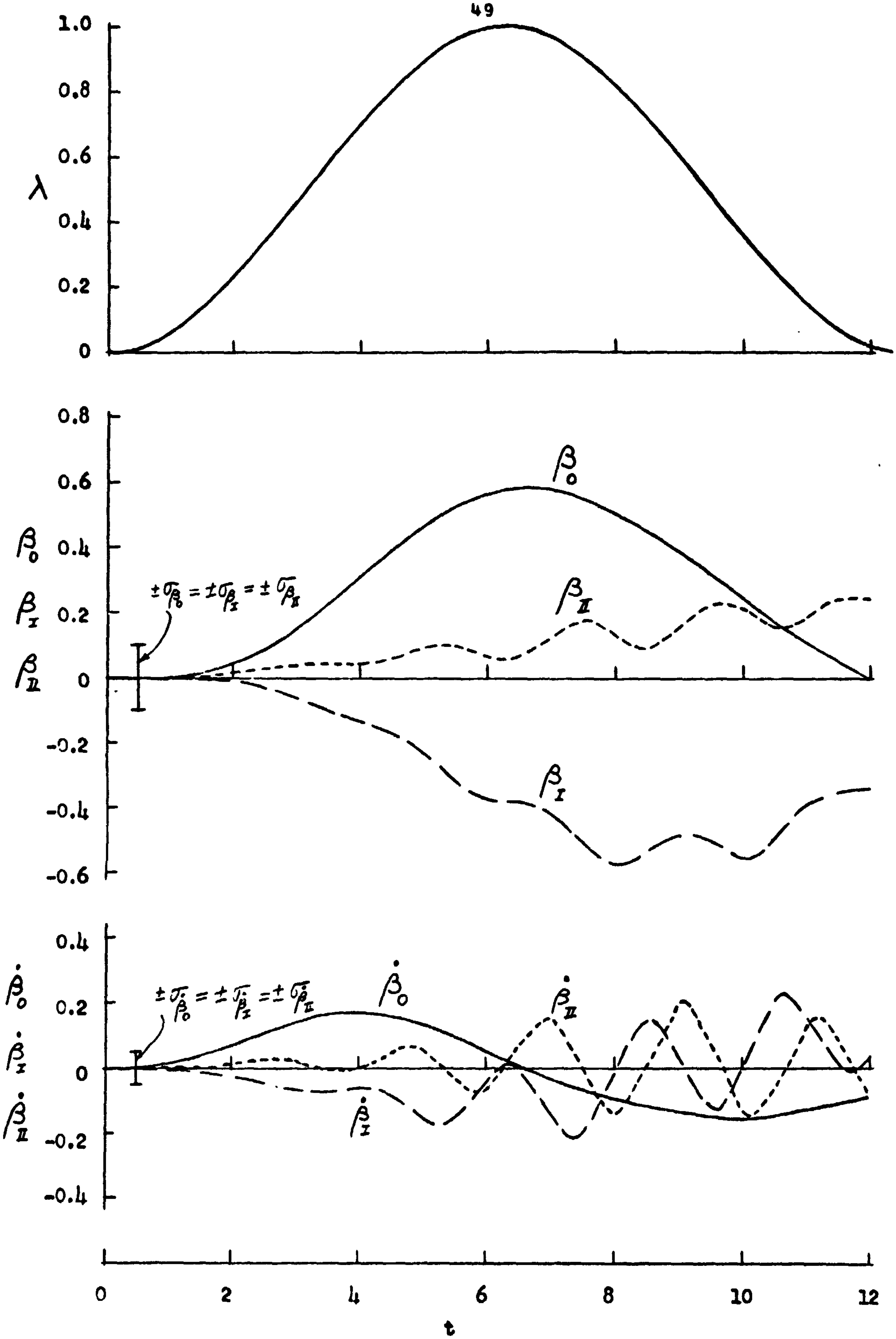

1.0
0.8
0.6
λ
0.4
0.2
0
0.8
0.6
0.4
0.2
0
-0.2
-0.4
-0.6
β_0
β_I
β_{II}
$\pm\sigma_{\beta_0} = \pm\sigma_{\beta_I} = \pm\sigma_{\beta_{II}}$
0.4
0.2
0
-0.2
-0.4
$\dot\beta_0$
$\dot\beta_I$
$\dot\beta_{II}$
$\pm\sigma_{\dot\beta_0} = \pm\sigma_{\dot\beta_I} = \pm\sigma_{\dot\beta_{II}}$
0
2
4
6
8
10
12
t

Fig. 11 (b)

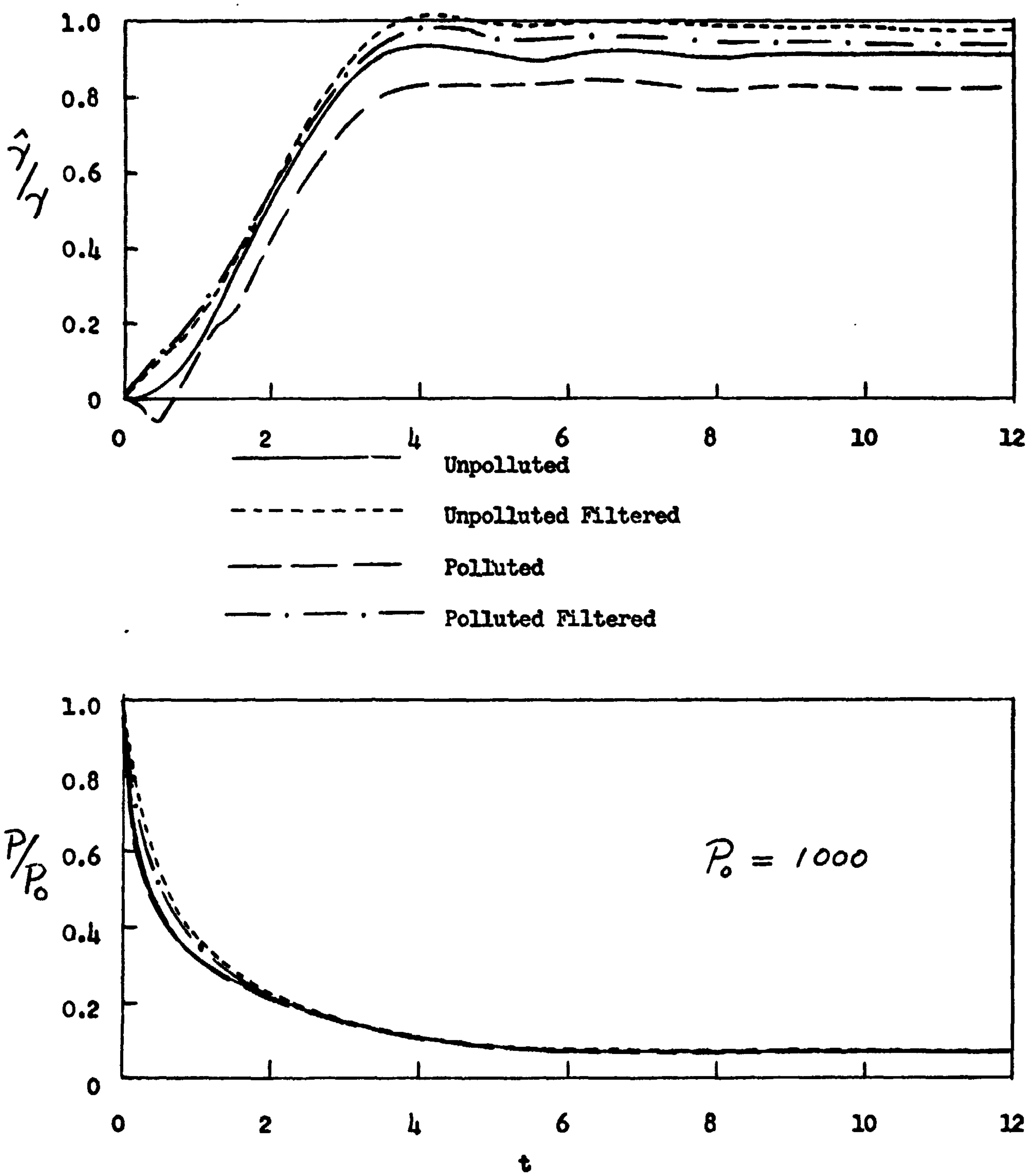
1.0
0.8
0.6
0.4
0.2
0
$\hat{\gamma}/\gamma$
0
2
4
6
8
10
12
Unpolluted
Unpolluted Filtered
Polluted
Polluted Filtered
1.0
0.8
0.6
0.4
0.2
0
P/P_o
$P_o = 1000$
0
2
4
6
8
10
12
t

Fig. 12 (a)

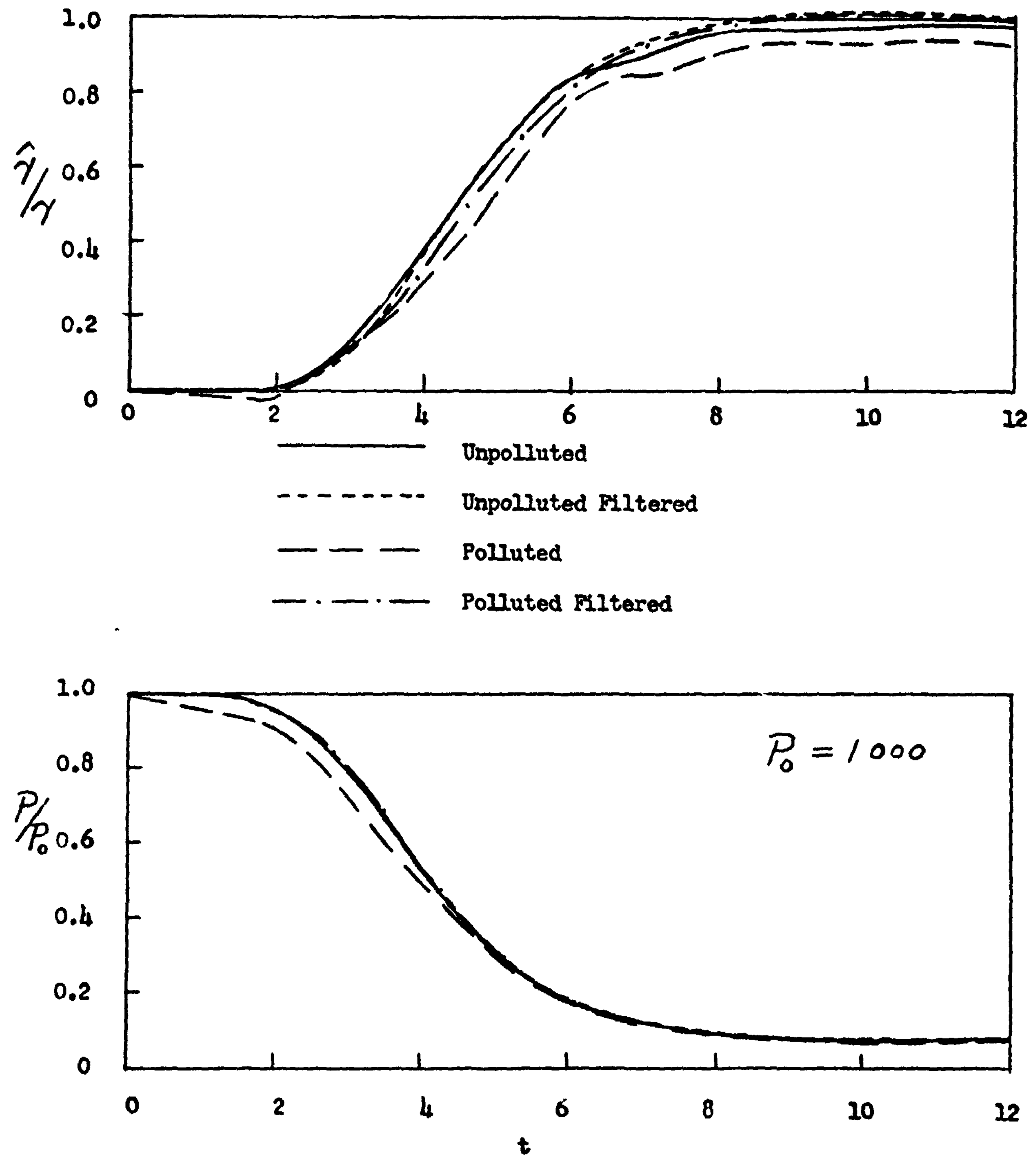
1.0
0.8
0.6
0.4
0.2
0
0
2
4
6
8
10
12
Unpolluted
Unpolluted Filtered
Polluted
Polluted Filtered
$\hat{\gamma}/\gamma$
P/P_o
$P_o = 1000$
t

Fig. 12 (b)

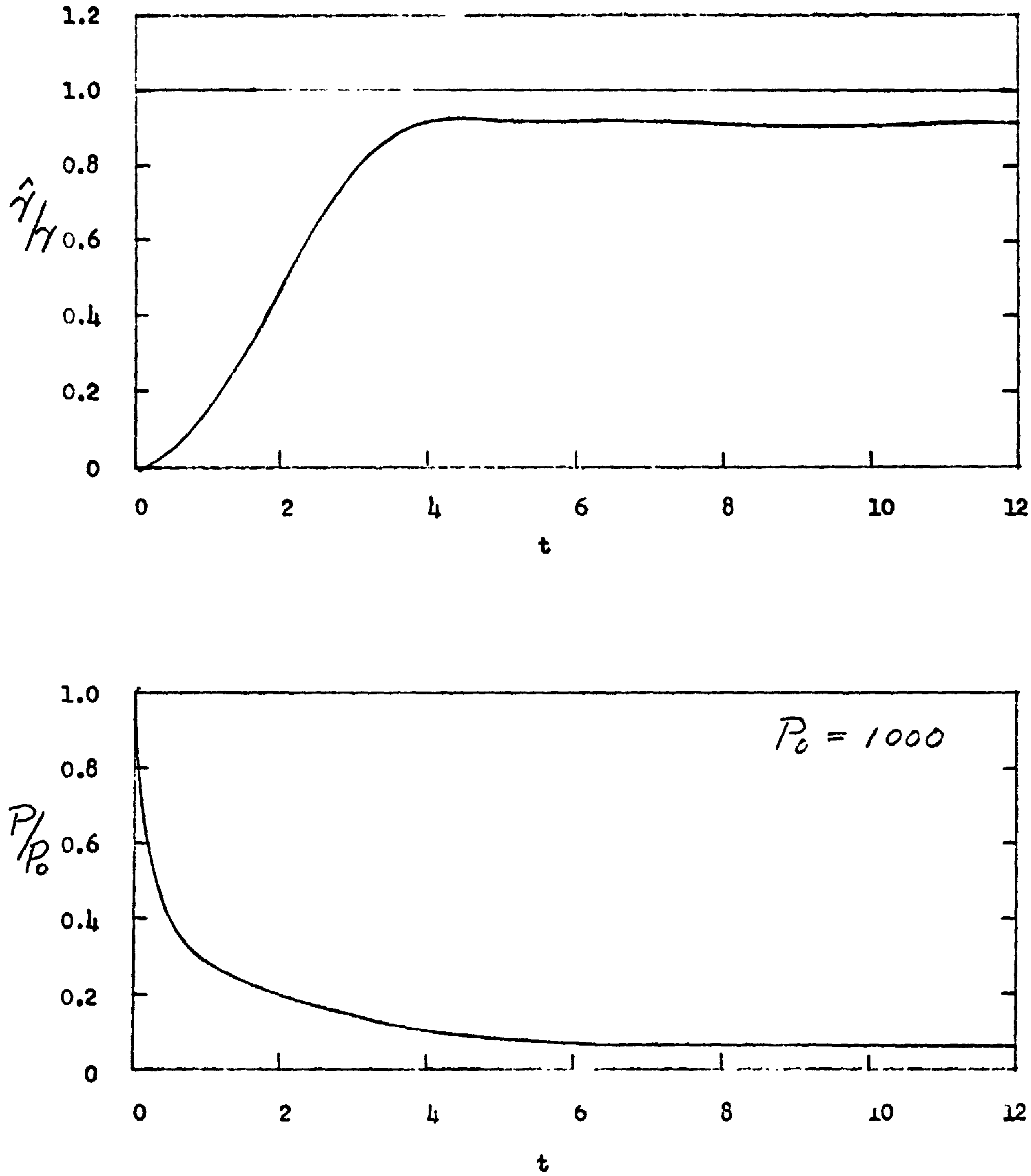
1.2
1.0
0.8
$\hat{\lambda}/\gamma$
0.6
0.4
0.2
0
0
2
4
6
8
10
12
t
1.0
$P_0 = 1000$
0.8
P/P_0
0.6
0.4
0.2
0
0
2
4
6
8
10
12
t

Fig. 13 (a)

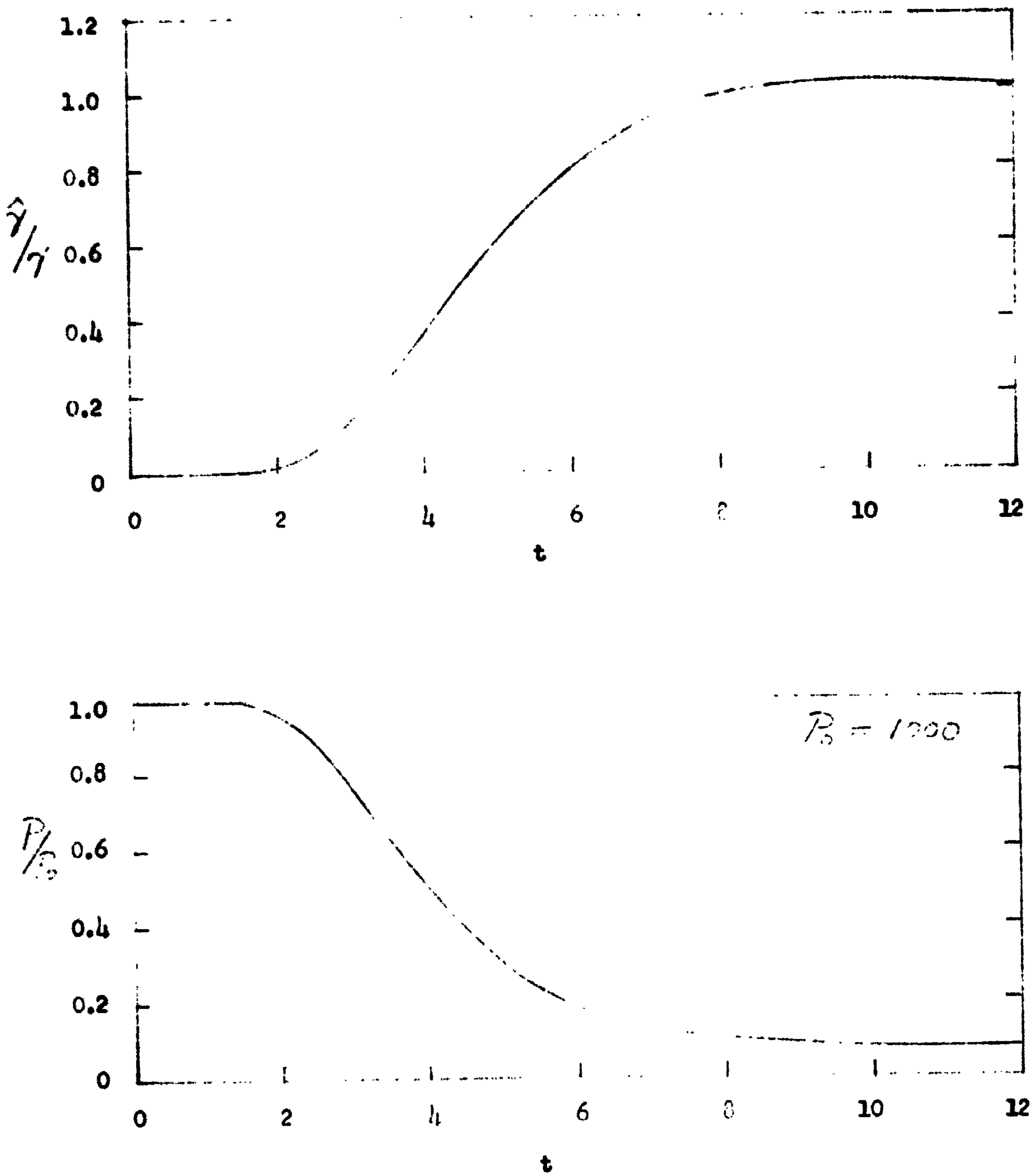
1.2
1.0
0.8
0.6
0.4
0.2
0
0
2
4
6
8
10
12
t
1.0
0.8
0.6
0.4
0.2
0
0
2
4
6
8
10
12
t
$P_0 = 1000$

Fig. 13 (b)